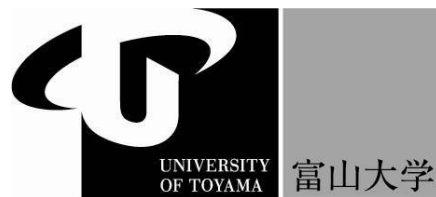


Working Paper No. 327

**A Statistical Model Connecting Heterogeneous Micro
Behaviors and Macrodynamics I : Construction
of a Basic Model and Its Nonlinear Analysis**

Akitaka Dohtani and Jun Matsuyama

October 2019



**SCHOOL OF ECONOMICS
UNIVERSITY OF TOYAMA**

Animal Spirits and Business Cycles I : A Dynamic Model and Its Nonlinear Analysis

by

Akitaka Dohtani and Jun Matsuyama

Faculty of Economics, University of Toyama

Gofuku 3190, Toyama, JAPAN

E-mail address: doutani@eco.u-toyama.ac.jp



TOYAMA
JAPAN

2019

Title: A Statistical Model Connecting Heterogeneous Micro Behaviors and Macrodynamics I : Construction of a Basic Model and Its Nonlinear Analysis

Subtitle: Business-cycle Model

Author: Akitaka Dohtani and Jun Matsuyama

Affiliation: Faculty of Economics, University of Toyama, 3190 Gofuku, Toyama 930, JAPAN.

E-mail address: doutani@eco.u-toyama.ac.jp

Abstract: We construct a simple Keynesian business cycles model in which animal spirits is incorporated into the model. We assume that each firm possesses the Keynesian investment function depending on demand. Like the well-known Kaldor model, we connect the animal spirits with the degree of response of investment to demand. However, for each firm we assume that even if the level of demand is the same, the strength of it is different between upswing and downswing of income. That is, we assume that the animal spirits of each firm is strong (resp. weak) in the case where demand increases (resp. decreases). This assumption implies that the Keynesian investment function of each firm is asymmetry. Unlike many Keynesian business cycles models, we introduce a certain kind of homogeneity among such a type of investment function. Moreover, we construct a statistical model that builds a bridge between micro-investment and macro-investment and derive a nonlinear macro-investment function. By using the investment function, we construct a simple business cycles model. We demonstrate that the nonlinearity yields a limit cycle in our model and detect the occurrence of a generalized Hopf bifurcation.

Keywords: Business Cycles; Animal Spirits; Density and Distribution functions; Asymmetric Investment Function; Poincaré-Bendixson Theorem; Generalized Hopf Bifurcation.

1. Introduction

The notion of animal spirits was introduced by John Maynard Keynes in his famous book: *General Theory of Employment, Interest*. In the book, Keynes states:

*Even apart from the instability due to speculation, there is the instability due to the characteristic of human nature that a large proportion of our positive activities depend on spontaneous optimism rather than mathematical expectations, whether moral or hedonistic or economic. Most, probably, of our decisions to do something positive, the full consequences of which will be drawn out over many days to come, can only be taken as the result of animal spirits—a spontaneous urge to action rather than inaction, and not as the outcome of a weighted average of quantitative benefits multiplied by quantitative probabilities.*¹

Akerlof and Shiller (2010) also states that the powerful forces of human psychology that are afoot in the world economy today. From various angles, Akerlof and Shiller (2010) discusses about the animal spirits. In the present paper, we are interested in the relation between the animal spirits and business cycles. At this early stage, one remark should be made. The main purpose of this paper is not to explain the *long-run* mechanism of determining animal spirits but to make clear the *short-run* mechanism that business cycles are produced by animal spirits. Especially, in the present paper, we stress on the importance of the word “a spontaneous urge to action rather than inaction”.

We construct a simple Keynesian business cycles model with the investment function that takes account of the animal spirits. Unlike Keynesian models, we distinguish between investment at a micro-level (i.e. investment of a firm) and that at a macro-level. We simply call the investment at a micro-level a micro-investment. On the other hand, we call the investment at a macro-level a macro-investment. We assume that each firm possesses micro-investment function depending on demand. The well-known examples of such an investment function are given by Kalecki (1935) and Kaldor (1940), although they consider a macro-investment function. Since Kalecki (1935) and Kaldor (1940) assume that each firm is homogeneous, the form of a macro-investment

¹ For this passage, see Keynes (1936, pp.161-162).

function is the same as that of a micro-investment function. Noting this point, following Kaldor (1940)², we here briefly explain Kaldor's idea of connecting the animal spirits with micro-investment function. Kaldor considers that the animal spirits is closely related to the degree (i.e. the slope of micro-investment function) of response of micro-investment to expected demand (income). The slope is called the marginal propensity to invest (abbreviated to MPI). For example, the animal spirits is strong (resp. weak) if MPI is large (resp. small). Kaldor assumed that MPI is large (resp. small) at a normal level (resp. lower and higher levels) of demand (therefore income).³ Thus, Kaldor considered that the strength of animal spirits depends on the absolute level of demand. However, we consider as follows. As Keynes states, a large proportion of our positive activities depends on spontaneous *optimism* rather than mathematical expectations. Animal spirits operates in the case where demand increases and both large-scale and small-scale micro-investments are executed. Consequently, MPI is large in the case. Conversely, animal spirits does not operate in the case where *demand decreases*. Then, since demand decreases, firms are pessimistic about the future economy and *small-scale micro-investments are executed but large-scale micro-investments are stopped*. Consequently, MPI is *small* in the case. Thus, the MPI in the case where demand increases is larger than that in the case where demand decreases and therefore, animal spirits introduces asymmetry (i.e. nonlinearity) into the MPI. We will show that such an asymmetry is a source of business cycles.

We first try to exclude the assumption that each firm is homogeneous. Then, we need a model that builds a bridge between micro-investments and a macro-investment. In the present paper, we first construct such a statistical model. By using the statistical model, a non-linear macro-investment function is derived from micro-level investments. Moreover, using the macro-investment function, we construct a simple two-dimensional discrete-time dynamic macro-model. To investigate the global dynamics of the discrete-time model, we construct a proxy continuous-time model. We prove that the above-mentioned nonlinearity yields stable business cycles. Since the macro-investment function is derived from the statistical argument, it becomes possible to statistically explain our results derived from the above dynamic model. This point will be an important contribution of the present paper. Needless to say, we also show that the

² The mathematical formulation of Kaldor model is given by Chang and Smyth (1971).

³ It has been well-known that this assumption introduces a sigmoid nonlinearity into the investment function and, as a result, yields business cycles. For example, see Asada (1987), Gabisch and Lorenz (1989), Owase (1991), and Lorenz (1993).

continuous-time model is sufficiently suitable as the proxy of the discrete-time model.

Our model is a simple two-dimensional continuous-time model and it allows a mathematically clear global analysis. We construct a square domain on whose boundary the vector field of our model points inward. If the equilibrium point is unstable, by using the Poincaré-Bendixson theorem⁴ we prove the occurrence of a limit cycle. The important feature of our model is that the existence domain of limit cycles is determined by a simple formula that is made up of model parameters (the marginal propensity to consume and the least upper and greatest lower bounds of MPI).

Moreover, we numerically show that there occurs a phenomenon that under very slight change of parameters, a limit cycle abruptly or discontinuously disappears at a parameter value. By using the above continuous-time model, we explain the mechanism of producing such a phenomenon. We also give an economic explanation of the phenomenon.

This paper is organized as follows. In Section 2, we construct a statistical model that builds a bridge between micro-investments and a macro-investment. In Section 3, we construct a two-dimensional discrete-time business cycle model of Keynesian type. In section 4, as a proxy of the discrete-time model, we construct a two-dimensional continuous-time model and provide a global dynamic analysis of the proxy model. In Section 5, we demonstrate the occurrence of the phenomenon that a limit cycle discontinuously disappears under a very slightly change of parameters. Moreover, we explain the mechanism of such a phenomenon. In Section 6, we demonstrate that the two-dimensional continuous-time model can be a true proxy of the original discrete-time model. Section 7 concludes, and Appendix contains the proofs of several results.

2. A Simple Statistical Model Connecting Micro and Macro

The model we consider in this paper is a Keynesian-type business cycle model. In order to accomplish one of our main purpose (the detection of limit cycles by using the Poincaré-Bendixson theorem), we need to construct as simply as possible. We define Y_n = income in period n , I_n = investment in period n , and C_n = consumption in period n . We employ the following consumption function: $C_n = \alpha Y_n + A$ ($1 > \alpha > 0$, $A > 0$).

⁴ For the Poincaré-Bendixson theorem, see Wiggins (1990, Section 1.1) and Medio and Lines (2001, Section 4.4.1).

On the other hand, like Kaldor (1940), we consider the macro-investment function: $I_n = iY_n - jK_n$ ($i > 0, j > 0$), where K_n = consumption in period n . In Sections 2 and 3, assuming $j = 0$, we construct a simple model without capital stock. In Section 4, we extend the simple model to the model with capital stock. Kaldor (1940) assumes that MPI is small at high and low levels of income and is large at a normal level of income. That is, MPI depends on income as described in Figure 1. The assumption makes the macro-investment function nonlinear. Kaldor (1940) and Chang and Smyth (1971) show that the nonlinearity yields limit cycles. For the nonlinear macro-investment function, the assumption that MPI is large in a normal range (in a neighborhood of the market equilibrium) represents that the animal spirits of firms intensifies in the range. Thus, in the above macro-investment function the animal spirits depends on income.

Figure 1 about here.

We will consider a macro-investment function that depends on the change of income. To make clear the relation between animal spirits and business cycles, we construct as a simple model as possible. So, we simply assume that the macro-investment linearly depends on income: $I_n = i_n Y_n$. As stated in Introduction, like Kaldor (1940) we consider that the animal spirits possesses an influence on MPI ($= i_n$) at period n . Kaldor (1940) assumed that the degree of influence depends on income. However, we assume that the degree of influence depends on the change of income. We consider the following MPI that depends on the change of income:

$$(2.1) \quad i_n = \Theta(u_n), \quad u_n \equiv Y_n - Y_{n-1}.$$

Equation (2.1) is the MPI of the macro-investment function. We call Eq. (2.1) the macro-MPI. Unlike Kaldor (1940), we try to introduce some kind of heterogeneity among firms. To do so, starting with the micro-investment function, we construct a statistical macro-investment function and give a theoretical explanation of (2.1). Moreover, we determine a typical form of the Θ -function.

Like the Kaldor model, we consider that for any firm, the production in period n equals the expected demand in period n . For simplicity, we assume that the set of firms is the continuum of $[0,1]$. Moreover, we assume that for a given u_n , the micro-investment function of the s -th firm ($s \in [0,1]$) in period n , is given by

$$I_n^s = i_n^s Y_n^s,$$

where Y_n^s ($s \in [0,1]$) is the production of (=the expected demand for) the s -th firm in period n .

Assumption 1: Y_n^s are Lebesgue measurable functions for $s \in [0,1]$.

Then, we have

$$Y_n = \int_{[0,1]} Y_n^s dm(s),$$

where m is the Lebesgue measure. We can regard i_n^s ($s \in [0,1]$) as the MPI of the s -th firm. We call it the micro-MPI. We here define

$$u_n^s \equiv Y_n^s - Y_{n-1}^s.$$

For simplification, we assume that each firm possesses two types of investment plan in the sense that the micro-MPI of each firm is given by

$$(2.2) \quad i_n^s \equiv \begin{cases} \rho_1^s & \text{if } u_n^s > \xi^s, \\ \rho_2^s & \text{if } u_n^s \leq \xi^s. \end{cases}$$

for some $\xi^s \in R^1$, where

$$(2.3) \quad \rho_1^s > \rho_2^s > 0.$$

It should be noted here that ξ^s may be negative. Inequality (2.3) implies that the micro-MPI in the case of $u_n^s > \xi^s$ becomes larger than that in the case of $u_n^s \leq \xi^s$. That is, Inequality (2.3) expresses that the investment of the s -th firm is active in the case of $u_n^s > \xi^s$ and inactive in the case of $u_n^s \leq \xi^s$. As stated in Introduction, this kind of asymmetry (i.e. nonlinearity) results from animal spirits. In the case of $\xi^s = 0$, the schematic dynamic behavior is described by Figure 2.

Figure 2 about here.

In the short run, it is natural that in the short run, the share of each firm is constant in the sense that there is an $\eta^s \in (0,1)$ such that

$$Y_n^s = \eta^s Y_n \quad \text{and therefore,} \quad u_n^s = \eta^s u_n.$$

Then, we have

Lemma 1: $1 = \int_{[0,1]} \eta^s dm(s).$ ■

Proof: From the definition, we have

$$Y_n = \int_{[0,1]} Y_n^s dm(s) = \int_{[0,1]} \eta^s Y_n dm(s) = Y_n \cdot \int_{[0,1]} \eta^s dm(s)$$

The proof follows directly from this result. ■

Throughout the remainder of Section 2, for simplicity we omit ‘ n ’. For example, we denote Y_n^s by Y^s . We assume that

Assumption 2: ρ_j^s ($j \in \{1,2\}$) and η^s are Lebesgue measurable functions for $s \in [0,1]$.

We define the following:

$$(2.4) \quad \Omega(u) \equiv \{s \in [0,1] : i^s = \rho_1^s \text{ (i.e. } u^s = \eta^s u > \xi^s)\}.$$

From the definition, we have the following result.

Lemma 2: The MPI of the s -th firm is given by

$$i^s \equiv \begin{cases} \rho_1^s & \text{if } s \in \Omega(u), \\ \rho_2^s & \text{if } s \in [0,1] \setminus \Omega(u). \end{cases} \blacksquare$$

Proof: Directly from the definition. ■

Assumption 3: $\Omega(u)$ is a Lebesgue-measurable set for any $u \in R^1$.

It is natural to assume the following.

Assumption 4: If $u < w$, then $\Omega(w) \supseteq \Omega(u)$ and $m(\Omega(w) - \Omega(u)) > 0$, where m is the Lebesgue measure,

Assumption 5: $\lim_{u \rightarrow -\infty} \Omega(u) = \emptyset$ and $\lim_{u \rightarrow \infty} \Omega(u) = [0,1]$,

where $A - B$ denotes the difference set between two sets A and B . Assumption 4 yields the following result:

Lemma 3: $\tilde{u}_n^s = \eta^s \tilde{u} > \xi^s$ for some $u = \tilde{u}$, then $u^s = \eta^s u > \xi^s$ for any macroeconomic changing rate $u > \tilde{u}$. ■

Proof: Directly from Assumption 4. ■

Lemma 1 implies that

if $i^s = \rho_1^s$ is employed (animal spirits is intensive) for some $u = \tilde{u}$, then $i^s = \rho_1^s$ (animal spirits remains intensive) is employed for any $u > \tilde{u}$.

From the definition (2.2) and Lemma 2, the macro-investment is given by

$$(2.5) \quad \begin{aligned} I &= \int_{\Omega(u)} \rho_1^s Y^s dm(s) + \int_{[0,1] - \Omega(u)} \rho_2^s Y^s dm(s) \\ &= \left\{ \int_{\Omega(u)} \rho_1^s \frac{Y^s}{Y} dm(s) + \int_{[0,1] - \Omega(u)} \rho_2^s \frac{Y^s}{Y} dm(s) \right\} Y \\ &= \left\{ \int_{\Omega(u)} \rho_1^s \eta^s dm(s) + \int_{[0,1] - \Omega(u)} \rho_2^s \eta^s dm(s) \right\} Y. \end{aligned}$$

We here define:

$$\Theta(u) \equiv \int_{\Omega(u)} \rho_1^s \eta^s dm(s) + \int_{[0,1]-\Omega(u)} \rho_2^s \eta^s dm(s).$$

Thus, we have

$$i = \frac{I}{Y} = \Theta(u).$$

Animal spirits is incorporated into the Θ – function. Our main purpose is that through the Θ – function, we consider the relation between animal spirits and business cycle. Therefore, it is convenient to introduce the following notion:

Definition 1: We call the value of $\Theta(u)$ social animal spirits (abbreviated to SAS) and the Θ – function a SAS function. ■

We here assume the following.

Assumption 6: The SAS function is a C^2 function.

As shown in the following, the SAS function makes it possible to carry out a statistical analysis that bridge between macro and micro. Through the statistical analysis, we present a new viewpoint concerning economic dynamics.

Using SAS function, we construct a distribution function. We start with the following lemma.

Lemma 4: We have

$$(2.6.1) \quad \text{if } u < w, \text{ then } \Theta(w) - \Theta(v) > 0,$$

$$(2.6.2) \quad \lim_{u \rightarrow +\infty} \Theta(u) = \int_{[0,1]} \rho_1^s \eta^s dm(s) \equiv \mu_1 = \text{the supremum of the SAS function,}$$

$$(2.6.3) \quad \lim_{u \rightarrow -\infty} \Theta(u) = \int_{[0,1]} \rho_2^s \eta^s dm(s) \equiv \mu_2 = \text{the infimum of the SAS function.} \blacksquare$$

Proof: See Appendix. ■

Lemma 5: $\Phi(u) = \frac{\Theta(u) - \mu_2}{\mu_1 - \mu_2}$ is a distribution function. ■

Proof: Directly from Lemma 4. ■

Lemma 5 also shows that $\Phi'(u)$ is a density function. The slope of the SAS function (i.e. the density function) is expected to be large in a small neighborhood of $u = 0$. In the following, we briefly explain the reason. It will be natural to consider as follows. In a small neighborhood of the point that u changes from $u < 0$ to $u > 0$, the economic situations of many firms change a turn for the better from $u^s(u) < 0$ to $u^s(u) > 0$. From the definition, this implies that as u changes from $u < 0$ to $u > 0$, the set $\Omega(u)$ becomes rapidly large and therefore, from the definition, the SAS function becomes rapidly large in the small neighborhood of $u = 0$. In other words, in the small neighborhood, the value of $\Phi'(u)$ (therefore, $\Theta'(u)$) is large. Especially, we later see that the height of $\Phi'(0)$ (therefore, $\Theta'(0)$) is closely related to instability of equilibrium.

Directly from Lemma 4, Lemma 4 determines the typical form of $\Theta(u)$.

Example 1: In this example, we give a simple explanation of above argument by using a normal distribution. We consider the distribution function of a normal distribution:

$$\Phi(u) = \frac{1}{3\sqrt{2\pi}} \int_{(-\infty, u]} \exp\left(-\frac{s^2}{18}\right) ds.$$

Moreover, Part (1) of Figure 3 describes the graph of the Φ -function. From the definition, we have the SAS function:

$$\Theta(u) = (\mu_1 - \mu_2)\Phi(u) + \mu_2 = \frac{(\mu_1 - \mu_2)}{3\sqrt{2\pi}} \int_{(-\infty, u]} \exp\left(-\frac{s^2}{18}\right) ds + \mu_2.$$

Part (2) of Figure 3 describes the graph of the SAS function with $\mu_1 = 0.2$ and $\mu_2 = 0.1$. ■

Figure 3 about here.

For simplicity, we work under the following assumption.

Assumption 7: $\Theta'(u)$ has a unique maximal point.

Clearly, we have

Lemma 6: $\Phi'(u)$ has a unique maximal point. ■

Proof: Directly from $\Theta''(u) = (\mu_1 - \mu_2)\Phi''(u)$ and Assumption 7. ■

We here introduce the following definition that plays an important role in giving statistical explanations of the main results.

Definition 2: We call $u = 0$ a macroeconomic turning point. We next define

$$u_{icp} = \{u \in R^1 : \Theta''(u) = 0\}$$

and call u_{icp} the most intensively changing point of animal spirits (abbreviated to MICPAS). ■

Since the maximal point of $\Phi'(u)$ is the same as that of $\Theta'(u)$, we obtain the following observation.

Observation 1: The MICPAS u_{icp} maximizes the changing rate of social animal spirits, $\Theta'(u)$. ■

We here give an intuitive explanation of the words “MICPAS and macroeconomic turning point”. We start with the explanation of macroeconomic turning point. Since u

denotes the change of Y , the macroeconomic turning point implies the turning point at which income changes from downswing to upswing. We next explain the MICPAS. From the definition, the MICPAS is the point at which the changing rate of SAS is maximal. That is, the MICPAS is the economic situation in which the degree of animal spirits in the whole economy rapidly increases. Therefore, at the MICPAS animal spirits spreads rapidly and widely.

As observed from Observation 1, it is expected that from a dynamic viewpoint, the location of the MICPAS has a great influence on the economic activity. In the following sections, using the SAS function that was derived through the above-mentioned statistical argument, we construct a business-cycle model and demonstrate this fact.

3. The Dynamic Model

Now, we start to construct a business-cycle model. Like the usual Keynesian business cycle models, we assume that

Assumption 8⁵: $1 > \alpha + \Theta(0)$.

Assumption 8 is assumed to guarantee the existence of a unique equilibrium. The same assumption has been employed in nonlinear Keynesian business-cycle models such as the Kaldor model. See for example Chang and Smyth (1971) and Lorenz (1993, Chapter 2). In the next section, we will prove that the degree of SAS becomes a source of business cycles by using a very simple dynamic model. From now on, we say a macro-investment function simply an investment function.

Lemma 5 demonstrates that the SAS function is asymmetric. In Example 1, we considered a SAS function that is derived by using a normal distribution. In analyzing the dynamic behavior, we however use merely the properties of SAS function, which is stated in Lemma 5. Therefore, in numerical examples, we use a simpler and more tractable SAS function than that defined by a normal distribution function. A typical example of such a SAS function is given in the following examples.

⁵ Assumption 7 implies that the marginal propensity to savings is larger than SAS at $u = 0$. The usual Keynesian business cycle model employs the same assumption. See also Lorenz (1993)

Example 3: From now on, in considering numerical examples, we use the SAS function, which is tractable:

$$(2.7) \quad \Theta(u) = a\text{Arctan}(bu + c) + d,$$

where we assume

$$(2.8) \quad d > a\pi/2, \quad 1 > d + a\pi/2.$$

Defining $\mu_1 = d + a\pi/2$ and $\mu_2 = d - a\pi/2$, we see that (2.7) possesses the properties of Lemma 5. The blue curve in Figure 4 describes the graph of the SAS function of (2.7) with $a = 0.03/\pi$, $b = 1/100$, $c = -1$, and $d = 0.12$. Clearly, these parameters satisfy (2.8). The greatest lower bound $\mu_2 = d - a\pi/2$ and the least upper bound $\mu_1 = d + a\pi/2$ of the SAS function are given by $0.12 + 0.015 = 0.135$ and $0.12 - 0.015 = 0.105$, respectively. The horizontal red lines in Figure 4 describe these bounds. It should be noted here that the asymmetry of the SAS function in this numerical example is very small. In the next section, we show that even this small asymmetry can be a source of business cycles. ■

Figure 4 about here.

Like many dynamic Keynesian models, the income is assumed to change as

$$Y_{n+1} - Y_n = \eta(I_n + C_n - Y_n) = \eta[\{\Theta(Y_n - Y_{n-1}) + \alpha - 1\}Y_n + A],$$

where $\eta > 0$ is an adjustment coefficient. For examples of the dynamic Keynesian models, see Kaldor (1940) and Goodwin (1951). See also Lorenz (1995). For simplicity, we assume that $\eta = 1$. Defining $Z_n = Y_{n-1}$, we have

$$A: \begin{cases} Y_{n+1} = \{\Theta(Y_n - Z_n) + \alpha\}Y_n + A, \\ Z_{n+1} = Y_n. \end{cases}$$

We start with the following Lemma.

Lemma 7: Suppose that Assumption 8 is satisfied. Then, System \mathcal{A} possesses a unique equilibrium point given by

$$(Y^*, Z^*) = \left(\frac{A}{1 - \alpha - \Theta(0)}, \frac{A}{1 - \alpha - \Theta(0)} \right). \blacksquare$$

Proof: Assumption 8 yields $1 - \alpha - \Theta(0) > 1 - \alpha - \mu_1 > 0$. From this, we can directly prove Lemma 7 from a simple calculation. \blacksquare

From Lemma 5, we see that the SAS function we consider is nonlinear. Before arguing the effects of such nonlinearity on dynamic behavior, we consider the case where the SAS function is constant.

Lemma 8: Suppose $\Theta(u) = \Theta_0$ (constant) and $1 > \alpha + \Theta_0$. Then System \mathcal{A} is globally asymptotically stable. \blacksquare

Proof: See Appendix. \blacksquare

In the case where the SAS function is nonlinear, it is not easy that we derive mathematically exact results concerning the difference equations system \mathcal{A} . Therefore, we here numerically demonstrate the occurrence of a invariant circle in System \mathcal{A} . In the next section, we rewrite System \mathcal{A} into a differential equations system and derive mathematically exact result.

See Figure 5. In Figure 5, we consider the same function as that of Example 2 and set $\alpha = 0.8$ and $A = 9900$. Figure 5 shows that System \mathcal{A} possesses a invariant circle that is given as the ω -limit set Γ_ω of a path of System \mathcal{A} . We define

$$Y(\theta) \equiv \frac{A}{1 - \alpha - \theta}, \quad \theta \in (0, 1 - \alpha).$$

Clearly, the Y -function is strictly increasing. Furthermore, we define

$$\Omega(\theta, \xi) \equiv [Y(\theta), Y(\xi)]^2.$$

See Figure 5. In Figure 5, we describe the boundary of $\Omega(\mu_2, \mu_1)$ by the red line.

Figure 5 shows that

$$(2.9) \quad \Gamma_\omega \subseteq \Omega(\mu_2, \mu_1).$$

In the next section, we suitably rewrite System Γ into a differential equations system and by using it, we exactly prove these facts on the dynamic behavior of the differential equations system Γ .

Figure 5 about here.

4. Analysis of Local and Global Dynamics in the Continuous-Time Version

In this section, we prove that the asymmetry of the SAS function yields business cycles. We start with the construction of a differential equations system that plays the role of a proxy of System A . To do so, we replace Y_n with a continuous-time variable $Y = Y(t)$. Moreover, we replace $Z_n = Y_{n-1}$ with a continuous-time variable $Z_p = Z_p(t)$ which satisfies

$$\dot{Z}_p = Y - Z_p.$$

Then, \dot{Z}_p becomes a proxy of $Y_n - Y_{n-1}$. We see later that (Y, Z_p) is sufficiently suitable for a proxy variable of (Y_n, Z_n) . Then, Eq. (2.1) is rewritten as

$$(3.1) \quad i = \Theta(u), \quad u = \dot{Z}_p.$$

We consider the same consumption function as that of Section 2. As usual, the discrete-time version of the dynamic mode concerning income is given by

$$\dot{Y} = \sigma(I + C - Y),$$

where $\sigma > 0$ is an adjustment coefficient. Like Section 2, For simplicity we assume

$$\sigma = 1.$$

Thus, we obtain a continuous-time model that is a proxy of System \mathcal{A} is given by

$$\Pi: \begin{cases} \dot{Y} = \{\Theta((Y - Z_p)) + \alpha - 1\}Y + A, \\ \dot{Z}_p = Y - Z_p. \end{cases}$$

In Section 5, we see in detail that System Π is sufficiently suitable for a proxy of System \mathcal{A} . As demonstrated immediately after, System Π makes it possible to completely analyze global dynamics of System \mathcal{A} . In the following, by using System Π , we prove the results on dynamic behavior, which are observed in Section 2. We first prove the following lemma concerning the existence and uniqueness of equilibrium.

Lemma 9: Suppose that Assumption 8 is satisfied. Then, System Π possesses the same equilibrium point as that of Lemma 7:

$$(Y^*, Z_p^*) = \left(\frac{A}{1 - \alpha - \Theta(0)}, \frac{A}{1 - \alpha - \Theta(0)} \right). \blacksquare$$

Proof: The proof is the same as that of Lemma 7. \blacksquare

Like Lemma 8 concerning the difference equations model \mathcal{A} , we prove the result on the global stability concerning the difference equations model Π .

Lemma 10: Under the same assumption as that of Lemma 8, System Π is globally asymptotically stable. \blacksquare

Proof: See Appendix. \blacksquare

In the case where the SAS function is non-constant, there is a possibility that the equilibrium point is unstable and therefore a limit cycle occurs. Before proving this, we analyze the dynamic behavior of System Π with a non-constant SAS function. The simplicity of System Π allows us to analyze the global dynamics. In fact, we can

construct a square domain on the boundary of which the vector field of System II points inwards. We prove the following lemma that determines the above square domain. Consequently, we prove the same result as (2.9).

Lemma 11: Suppose that Assumption 8 is satisfied. Then, the closed set $\Omega(\mu_2, \mu_1)$ is positively invariant. Moreover, for the solution $P(t) = (Y(t), Z_p(t))$ starting at a point in $\text{ext}\Omega(\mu_2, \mu_1)$, we have

$$\Gamma_\omega \subseteq \Omega(\mu_2, \mu_1),$$

where Γ_ω is the ω -limit set of $P(t)$. ■

Proof: See Appendix. See Figure 5, Figure 5 describes that the rectangular domain in Figure 5 is an attracting set⁶. In the appendix, we prove the observation. ■

We now examine the occurrence of limit cycles in System II. From Lemma 11, the instability of the equilibrium point guarantees the occurrence of a limit cycle. The following assumption guarantees the instability of the equilibrium point.

Assumption 9: $\{2 - \Theta(0) - \alpha\} \{1 - \alpha - \Theta(0)\} < A\Theta'(0)$.

If $(2 - \alpha)(1 - \alpha) < A\Theta'(0)$ is satisfied, then Assumption 9 is satisfied. Therefore, $\Theta'(0)$ is large, then there is a high possibility that Assumption 9 is satisfied. We now prove that Assumption 9 guarantees the local instability of the equilibrium point.

Theorem 1: Suppose that System II satisfies Assumptions 7 and 8. Then, it follows that the equilibrium point of System II is completely unstable in the sense that the real parts of the eigenvalues of the Jacobian matrix estimated at the equilibrium point are positive. ■

Proof: See Appendix. ■

Thus, we obtain the following main theorem on the occurrence of a limit cycle.

⁶ For the notion of attracting set, see Perko (1996, P.193).

Theorem 2: Suppose that Assumptions 7 and 8 are satisfied. Then, it follows that any non-trivial⁷ path of System Π converges to a non-trivial limit cycle in $\Omega(\mu_2, \mu_1)$. ■

Proof: The proof of Theorem 2 follows directly from the Poincaré-Bendixson theorem, Lemma 10, and Theorem 1. ■

From Theorem 2, we find that

the existence domain of a limit cycle is determined by the supremum μ_1 and the infimum μ_2 of the SAS function.

This result is the most remarkable feature of our model. Thus, we prove that even small asymmetry of SAS function, which is caused by the animal spirits, can be a source of business cycles.

By using numerical examples, we will consider a various type of dynamic behavior. In considering it, we use the SAS function given by (2.7). So, for System Π with such a SAS function, we prove the following lemma that is useful in determining the stability of equilibrium.

Lemma 12: We consider the SAS function of (3.1). The stability of the equilibrium point is give as follows.

(3.2.1) If $H(a, b, c, d, \alpha, A) > 2$, Assumption 9 is satisfied and the equilibrium point is completely unstable;

(3.2.2) If $H(a, b, c, d, \alpha, A) < 2$, the equilibrium point is asymptotically stable,

where

$$\begin{aligned} H(a, b, c, d, \alpha, A) &\equiv \frac{abA}{(c^2 + d)\{1 - \alpha - \Theta(0)\}} + \Theta(0) + \alpha. \\ &\equiv \frac{abA}{(c^2 + d)\{1 - \alpha - a\text{ArcTan}(c) - d\}} + a\text{ArcTan}(c) + d + \alpha. \blacksquare \end{aligned}$$

Proof: See Appendix. ■

⁷ The word “non-trivial path” implies the “non-equilibrium point”.

We now provide numerical examples in which (3.2.1) is satisfied and System Π possesses a stable limit cycle.

Example 4: We consider the case in which the SAS function is given by (2.7). Except for a , b , c and d , we consider the same parameter values as those of Figure 5. We set

$$(a, b, c, d) = (0.03/\pi, 1/100, 1, 0.12).$$

Then, the SAS function satisfies Assumptions 7 and 8. We have

$$H(0.03/\pi, 1/100, 1, 0.12, 0.8, 9900) > 4 > 2.$$

Therefore, from (3.2.1) it directly follows that the equilibrium point is completely unstable. The blue path in Figure 6 describes the maximal limit cycle of System Π . The limit cycle turns counterclockwise. We have

$$\begin{aligned} \mu_2 &= -\frac{a\pi}{2} + d = 0.105, & \mu_1 &= \frac{a\pi}{2} + d = 0.135, \\ Y(\mu_2) &= \frac{A}{1-\alpha-\mu_2} = \frac{9900}{0.095}, & Y(\mu_1) &= \frac{A}{1-\alpha-\mu_1} = \frac{9900}{0.065}, \\ \Omega(\mu_2, \mu_1) &= \left[\frac{9900}{0.095}, \frac{9900}{0.065} \right]^2. \end{aligned}$$

The red square in Figure 6 describes $\partial\Omega(\mu_2, \mu_1)$, where ∂A is the boundary of the set A . Figure 6 also describes the results of Theorem 2 on the dynamic behavior in the exterior of the maximal limit cycle. That is, any solution starting at a point in $\text{ext}\Omega(\mu_2, \mu_1)$ enters $\Omega(\mu_2, \mu_1)$ and stays in it. Figure 6 indicates that $\Omega(\mu_2, \mu_1)$ determines the existence domain of limit cycles. The nonlinearity function of System Π is incorporated into the SAS function, only. As stated in Example 2, since $\mu_1 - \mu_2 = 0.03$, the nonlinearity of the SAS function in this example is very small. Nevertheless, our result and Figure 6 show that even this small nonlinearity can be a source of business cycles.

Figure 6 about here.

Lemma 11 and Figure 6 suggest that we obtain the information on the amplitude of the maximal limit cycle from the size of $\mu_1 - \mu_2$, and that we obtain the information on the location of the maximal limit cycle from the magnitudes of μ_2 and μ_1 . For these points, see Figure 7. We set $(b, c) = (1/100, 1)$. Blue and red curves in Part (1) of Figure 7 describe the asymmetric SAS function with $(a, d) = (0.04/\pi, 0.13)$ and $(a, d) = (0.03/\pi, 0.1)$, respectively. We have

$$\begin{aligned} H(0.04/\pi, 1/100, 1, 0.13, 0.8, 9900) &> 5 > 2, \\ H(0.03/\pi, 1/100, 1, 0.1, 0.8, 9900) &> 3 > 2. \end{aligned}$$

Therefore, it follows directly from Lemma 12 that in both cases the equilibrium point is completely unstable. Thus, Theorem 2 establishes the occurrence of an externally stable limit cycle. Blue and red cycles in Part (2) of Figure 7 describe the maximal limit cycles in the cases of the blue and red curves of Part (1) of Figure 7, respectively. The red squares of Part (2) describe $\partial\Omega(\mu_2, \mu_1)$ that determines the existence domain of limit cycles at $(a, d) = (0.04/\pi, 0.13)$ and $(a, d) = (0.03/\pi, 0.1)$, respectively. In the same calculation as above, the upper and the lower red squares are respectively given by

$$\Omega(\mu_2, \mu_1) = \left[\frac{9900}{0.09}, \frac{9900}{0.05} \right]^2, \quad \Omega(\mu_2, \mu_1) = \left[\frac{9900}{0.115}, \frac{9900}{0.085} \right]^2.$$

Figure 7 indicates that as $\mu_1 - \mu_2$ is large, the amplitude of the maximal limit cycle is large, and as the magnitudes of both μ_2 and μ_1 are large, the maximal limit cycle is located at the upper left. ■

Figure 7 about here.

5. Abrupt Disappearance or Appearance of a Limit Cycle: Generalized Hopf Bifurcation

In this section, we numerically demonstrate the occurrence of the phenomenon that a limit cycle abruptly disappears at a parameter value. See Figures 8 and 9. In Figures 8 and 9, we consider the SAS function defined by (2.6) and set $\alpha = 0.82$, $a = 0.03/\pi$, $b = 1/100$, and $d = 0.1$. We define

$$c_1 = -3.2 \quad \text{and} \quad c_2 = -2.992.$$

Red and blue curves of Figure 8 describe the SAS functions with $c = c_1$ and $c = c_2$, respectively. It should be noted here that two curves are almost the same. That is, the difference between two SAS functions is very small. On the other hand, Parts (1) and (2) of Figure 9 describe paths of System II with $c = c_1$ and $c = c_2$, respectively. The starting points of paths of Parts (1) and (2) are the same. The change from $c = c_1$ to $c = c_2$ (from $c = c_2$ to $c = c_1$) produces the abrupt disappearance (resp. the abrupt creation) of limit cycle. Figures 8 and 9 suggest the occurrence of the above-mentioned phenomenon.

Figures 8 and 9 about here.

Except for the value of c , we set the same parameter values as those given in Figure 9. We start with the following lemma concerning the stability of the equilibrium.

Lemma 13: Suppose that System II satisfies Assumptions 7 and 8. For any $c \in [c_1, c_2]$, the equilibrium of System II is asymptotically stable. ■

Proof: See Appendix. ■

Figure 10 describes the paths of System II with the parameter values given in Part (1) of Figure 9. Blue and red curves in Figure 10 describe the paths of System II with

$$(Y(0), Z_p(0)) = (108670, 108820), \quad (Y(0), Z_p(0)) = (108670, 108600),$$

respectively. The paths turn counterclockwise. Figure 10 shows that the blue path converges to a stable limit cycle but the red path converges to the equilibrium point. Consequently, Figure 10 indicates that System II yields not only a stable limit cycle but also an unstable limit cycle in which corridor stability⁸ occurs.

Figure 10 about here.

⁸ For the notion of corridor stability, see Leijonhufvud (1973), and for the mathematical interpretation of corridor stability, see Benhabib and Miyao (1981).

We now make one important observation. As stated above, a slight change in parameter c from c_1 to c_2 yields a great change in dynamic behavior: All the limit cycles disappear abruptly (discontinuously) and the system becomes globally stable. Why does such a phenomenon occur? We show that this seemingly strange phenomenon is closely related to the occurrence of a generalized Hopf bifurcation and the appearance of a transient cycle-like behavior. Figure 10 shows that

(i) The maximal limit cycle at $c = c_1$ is stable.

Figure 10 also shows the occurrence of corridor stability. That is,

(ii) At $c = c_1$, a minimal limit cycle exists such that any path in the interior of the minimal limit cycle converges to the equilibrium point.

Moreover, Figure 10 shows that

(iii) The limit cycle at $c = c_1$ (immediately before $c = c_2$ when all cycles disappear discontinuously) is not small.

This implies that global stability does not result from the contraction and crush of the maximal cycle. In Figure 11, we consider the case of $c_3 = 3.566606 \in]c_1, c_2[$ and choose, except for the value of c , the same parameter values as given in Figure 9. In this case, Lemma 13 indicates that the equilibrium is asymptotically stable. Therefore, from Lemma 10 it directly follows that the equilibrium point is asymptotically stable. Parts (1) and (2) of Figure 11 describe a path of System II and its time series, respectively. The figure shows that although the path ultimately converges to the equilibrium point, it behaves like a limit cycle in the course of convergence, whose form is almost the same as the maximal limit cycle at $c = c_1$. Thus, at $c = c_3$ (immediately after the system becomes globally stable), we obtain the following:

(iv) The system possesses a long transient cycle-like behavior.

(v) The long transient cycle-like behavior resembles the maximal cycle at $c = c_1$.

With (i) to (v), we can provide a typical process that yields global stability immediately after the abrupt and discontinuous disappearance of limit cycles. First, the system possesses at least two limit cycles, the maximal stable limit cycle and the minimal unstable limit cycle. As the parameter c increases, these limit cycles approach and coincide to yield a semi-stable cycle. This situation is structurally unstable. Therefore, as c becomes large, the semi-stable cycle abruptly disappears and the system becomes globally stable. Thus, the above dynamic phenomena occur through this process.

Figure 11 about here.

However, this does not explain the transient cycle-like behavior described in Figure 11. To explain this, we first describe the above transition process by using the (Poincaré) return map⁹. We start with the construction of the return maps, which show the abrupt disappearance of limit cycles and the occurrence of global stability. By c^* , we denote the value of c at which the semi-stable cycle appears. In the ε -neighborhood $W \equiv]c^* - \varepsilon, c^* + \varepsilon[$ of c^* , we construct a return map $\Gamma : V \rightarrow R^1$. Using the return map, we substitute the dynamic behavior of our continuous-time model with that of the discrete-time system: $u_{n+1} = \Gamma(u_n)$. A fixed point of the discrete-time system corresponds to a periodic solution of our continuous-time model. In particular, if the derivative estimated at the fixed point is larger than 1 (smaller than 1), then the corresponding periodic solution is stable (unstable). Moreover, if the derivative equals 1 (i.e., the graph of the return map is tangent to the 45° line) and the second derivative is nonzero, then the corresponding periodic solution is semi-stable.

Part (1) of Figure 12 describes three schematic graphs of the return maps, which describe the above phenomena. The black straight lines in Parts (1) and (2) are the 45° lines, and the origins in Parts (1) and (2) correspond to the equilibrium point of System II. The brown curve in Part (1) of Figure 12 describes the graph of the return map at $c = c_1 (< c^*)$. In this case, the return map possesses lower, medium, and upper equilibria. The lower equilibrium is the origin. The medium and the upper equilibria are unstable and stable and correspond to the stable and the unstable limit cycles, respectively. Moreover, the blue curve in Part (1) describes the graph of the return map at $c = c^*$. In this case, the return map possesses lower and upper equilibria. The upper equilibrium is

⁹ For a detailed explanation of the (Poincaré) return map or first-return map, see Pontryagin (1962). See also Wiggins (1990), Glendinning (1994) and Medio and Lines (2001, Section 4.4.1).

semi-stable and corresponds to the semi-stable cycle. Finally, the red curve in Part (1) describes the graph of the return map at $c = c_2 (> c^*)$. In this case, the equilibrium point of the return map is only one (the origin) and globally stable. Thus, Part (1) describes the above-mentioned abrupt and discontinuous disappearance of limit cycles after the coincidence of stable and unstable limit cycles. Thus, Part (1) provides a schematic return-map description of the above transition process. The bifurcation described in Part (1) is called a *fold bifurcation* (often called a *saddle-node bifurcation*).¹⁰ The continuous-time version of the fold bifurcation is called a generalized Hopf bifurcation. From Lemma 13, the equilibrium is asymptotically stable throughout the above transition process. Therefore, in the above transition process of dynamic behavior, such a generalized Hopf bifurcation is different from the standard Hopf bifurcation.

On the other hand, using the return map, we obtain a clear description of the close relationship between the generalized Hopf bifurcation and the long transient cycle-like behavior. The red curve in Part (2) of Figure 12 describes the graph of the return map at $c = c_3 (> c^*)$ sufficiently near to c^* . As described in Part (2), such a return map possesses a part very close to the 45° line. In such a part, the return map behaves like an equilibrium point (see Part (2) of Figure 12). Therefore, the corresponding path of the original continuous-time model behaves like a limit cycle for a long time. However, as described in Part (2), the path ultimately converges to the origin and, therefore, the corresponding path of System II converges to the equilibrium point. In this sense, the generalized Hopf bifurcation is closely related to the long transient cycle-like behavior. Based on these observation, we can conclude that the abrupt and discontinuous disappearance of limit cycles and the long transient cycle-like behavior results from the generalized Hopf bifurcation.

Figure 12 about here.

6. Suitability of Proxy Variable

In this section, we see that System II is sufficiently suitable as a proxy of the difference equations system A. We start from a similarity between the paths of two

¹⁰ See Glendinning (1994, Section 8.3) and Medio and Lines (2001, Section 4.4.1).

systems. In Section 3, we already saw that both systems yield persistent business fluctuations which are included in $\Omega(\mu_2, \mu_1)$. See Figures 5 and 6. Parts (1) and (2) of Figure 13 describes the time series of paths of Systems A and II , respectively. For Systems II and A of Figure 13, we set the same parameter values as those of Figures 5 and 6, respectively. Therefore, in Figure 13, the parameter values of Part (1) are the same as those of Part (2). Especially, the starting point of the path of Part (1) is the same as that of Part (2). Figure 13 demonstrates that a path of the original discrete-time system A is almost the same as a path of the continuous-time proxy system II . Thus, Figure 13 shows that System II is a sufficiently suitable proxy of System A .

On the other hand, in Section 5, we saw that System II causes the abrupt disappearance or the abrupt creation of a limit circle. We numerically see that System A also causes a similar phenomenon. See Figure 14. In Figure 14, except for the value of c , we set the same parameter values as those of Figure 11. Parts (1) and (2) of Figure 13 describes the time series of paths of System A with $c = 3.1564891$ and $c = 3.1564892$, respectively. Two paths have the same starting point. Thus, Figure 14 demonstrates that from the quantitative viewpoint, System II is sufficiently suitable as a proxy of System A .

Figures 13 and 14 about here.

7. Conclusions

In this paper, following a Keynes' suggestion in his famous book, we considered we considered the short-run relation between animal spirits and business cycles. Like Kaldor (1940), we assumed that animal spirits possesses an effect on MPI. We assumed that the degree of influence depends on the change of income. The reason is as follows. If the change of income is positive, animal spirits operates (both large-scale and small-scale investments are executed) and the SAS function is large. Conversely, if the change of income negative, animal spirits does not operate (small-scale investments are executed but large-scale investments are stopped) and the SAS function is small. We demonstrated that this simple investment behavior creates business cycles. Based on the observation, we constructed an investment function at a micro-level. Next, we construct a statistical model that bridges between a micro-level and a macro-level and through a

statistical argument, we provided a macro-level investment function. The investment function possesses the SAS function that is closely related to a distribution function.

We incorporated the investment function with the SAS function into a disequilibrium dynamic model with the Keynesian consumption function. We demonstrated that the dynamic model of Keynesian type yields business cycles.

Our original model is a two-dimensional discrete-time model. As a proxy of the discrete-time model, we constructed a two-dimensional continuous-time model that allows us to determine detailed global dynamics. We also derived a square domain determined by parameters of our model, in which any path enters. As a result, in the case where the equilibrium point is completely unstable, by using the Poincare-Bendixson Theorem, we proved the occurrence of business cycles.

We numerically showed a phenomenon that under a slight change of a parameter, limit cycles abruptly disappear and global stability dominates. We numerically demonstrated that in the case where the equilibrium point is stable, the phenomenon is created by the coincidence of outer stable limit cycle and inner unstable limit cycle. Thus, we see that such a phenomenon results from the generalized Hopf bifurcation that is different from the Hopf bifurcation. In the neighborhood of such a phenomenon, we also observed a long transient cycle-like dynamic behavior. The emergence of such a dynamic behavior is also a feature of the generalized Hopf bifurcation.

Finally, we demonstrated that the proxy continuous-time model is sufficiently suitable as a proxy of the original discrete-time model. From a qualitative viewpoint, we saw that any path of the original model enters into the same square domain as that of the proxy model. Therefore, in the case where the equilibrium point is completely unstable, all invariant circles emerges in the square. Moreover, we demonstrated that like the proxy model, the original model also has the phenomenon that under a very slight change of a parameter, invariant circles the abruptly disappear and global stability dominates. We also demonstrated that the dynamics resulting from the shifts of MICPAS are very similar in both systems.

As observed from phase diagrams provided in this paper (see Figures 6 and 7), both discrete-time and continuous-time systems possess strong attractions to a neighborhood of the equilibrium. This suggests that our results obtained in this paper are robust under modifications and extensions, although we must leave the confirmation of it as a future research.

8. Appendix

In this appendix, we provide the proof of several lemmas and Theorem 1. We start with the well-known Olech theorem.

Proof of Lemma 4: We assume $w > u$. Assumption 4 yields $\Omega(w)^C \cap \Omega(u) = \phi$. Therefore,

$$\begin{aligned}
 (9.1) \quad \{[0,1] - \Omega(w)\} - \{[0,1] - \Omega(u)\} &= \{[0,1] \cap \Omega(w)^C\} \cap \{[0,1] \cap \Omega(u)^C\}^C \\
 &= [0,1] \cap \Omega(w)^C \cap \{[0,1]^C \cup \Omega(u)\} \\
 &= \{[0,1] \cap \Omega(w)^C \cap [0,1]^C\} \\
 &\quad \cup \{[0,1] \cap \Omega(w)^C \cap \Omega(u)\} \\
 &= [0,1] \cap \Omega(w)^C \cap \Omega(u) = \Omega(w)^C \cap \Omega(u) = \phi.
 \end{aligned}$$

Noting Assumption 2, we define

$$\begin{aligned}
 \rho_1^{\min} &\equiv \min\{\rho_1^s : s \in [0,1]\} > 0, \quad \rho_1^{\max} \equiv \max\{\rho_1^s : s \in [0,1]\} > 0 \\
 \rho_2^{\min} &\equiv \min\{\rho_2^s : s \in [0,1]\} > 0, \quad \eta_{\min} \equiv \min\{\eta^s : s \in [0,1]\} > 0, \\
 \text{and } \eta_{\max} &\equiv \max\{\eta^s : s \in [0,1]\} > 0
 \end{aligned}$$

Therefore, we see from (9.1) and Assumption 4 that

$$\begin{aligned}
 (9.2) \quad \Theta(w) - \Theta(u) &= \int_{\Omega(w)} \rho_1^s \eta^s dm(s) + \int_{[0,1] - \Omega(w)} \rho_2^s \eta^s dm(s) \\
 &\quad - \int_{\Omega(u)} \rho_1^s \eta^s dm(s) - \int_{[0,1] - \Omega(u)} \rho_2^s \eta^s dm(s) \\
 &= \int_{\Omega(w) - \Omega(u)} \rho_1^s \eta^s dm(s) + \int_{\{[0,1] - \Omega(u)\} - \{[0,1] - \Omega(w)\}} \rho_2^s \eta^s dm(s) \\
 &= \int_{\Omega(w) - \Omega(u)} \rho_1^s \eta^s dm(s) > \rho_1^{\min} \eta_{\min} \bullet m(\Omega(w) - \Omega(u)) > 0.
 \end{aligned}$$

This proves Equation (2.6.1). On the other hand,

$$\begin{aligned}
\Theta(u) &= \int_{\Omega(w)} \rho_1^s \eta^s dm(s) + \int_{[0,1]-\Omega(w)} \rho_2^s \eta^s dm(s) \\
&\leq \int_{\Omega(w)} \rho_1^s \eta^s dm(s) + \int_{[0,1]-\Omega(w)} \rho_1^s \eta^s dm(s) \\
&= \int_{[0,1]} \rho_1^s \eta^s dm(s) \leq \rho_1^{\max} \eta_{\max}, \\
\Theta(u) &= \int_{\Omega(w)} \rho_1^s \eta^s dm(s) + \int_{[0,1]-\Omega(w)} \rho_2^s \eta^s dm(s) \\
&\geq \int_{\Omega(w)} \rho_2^s \eta^s dm(s) + \int_{[0,1]-\Omega(w)} \rho_2^s \eta^s dm(s) \\
&= \int_{[0,1]} \rho_2^s \eta^s dm(s) \geq \rho_2^{\min} \eta_{\min}
\end{aligned}$$

Since (2.6.1) shows that the SAS function is strictly monotonous, these two inequalities yield Equations (2.6.2) and (2.6.3). Thus, we complete the proof. ■

Proof of Lemma 8: From the assumption, the system becomes

$$A: \begin{cases} Y_{n+1} = \{\Theta_0 + \alpha\}Y_n + A, \\ Z_{n+1} = Y_n. \end{cases}$$

Since $1 > \alpha + \Theta_0$, we see that

$$\lim_{n \rightarrow \infty} Y_n = A/(1 - \alpha - \Theta_0) = Y^* = \lim_{n \rightarrow \infty} Z_n.$$

This complete the proof. ■

Olech Theorem: Suppose that the following system possesses an equilibrium point.

$$\Sigma \begin{cases} \bullet \\ w = F(w, z), \\ \bullet \\ z = G(w, z). \end{cases}$$

The equilibrium point is globally asymptotically stable (i.e., the equilibrium point is stable and any path converges to the equilibrium point), under the following conditions:

- (O.1) $\partial F / \partial w + \partial G / \partial z < 0$ for any $(w, z) \in R^2$;
- (O.2) $\partial F / \partial w \bullet \partial G / \partial z - \partial F / \partial z \bullet \partial G / \partial w > 0$ for any $(w, z) \in R^2$;
- (O.3) $\partial F / \partial w \bullet \partial G / \partial z \neq 0$ or $\partial F / \partial z \bullet \partial G / \partial w \neq 0$ for any $(w, z) \in R^2$. ■

Proof: See Olech (1963). ■

Proof of Lemma 10: We have the following Jacobian matrix of System II .

$$J(Y, Z_p) = \begin{bmatrix} \Theta'(\beta(Y - Z_p))Y + \Theta(\beta(Y - Z_p)) + \alpha - 1 & -\Theta'(\beta(Y - Z_p))Y \\ 1 & -1 \end{bmatrix}.$$

Since $Y^* = Z_p^* = A / \{1 - \alpha - \Theta(0)\}$, the Jacobian matrix estimated at the equilibrium point is given by

$$(9.3) \quad J(Y^*, Z_p^*) = \begin{bmatrix} \Theta'(0)Y + \Theta(0) + \alpha - 1 & -\Theta'(0)Y \\ 1 & -1 \end{bmatrix}.$$

Define $\Theta(0) = c \in (0, 1)$. Then, since the SAS function is constant, $\Theta'(0) = 0$. Therefore, the Jacobian matrix of System II is given by

$$J(Y^*, Z_p^*) = \begin{bmatrix} -\{1 - \Theta(0) - \alpha\} & 0 \\ 1 & -1 \end{bmatrix}.$$

From the assumption of Lemma 10, we have $1 - \Theta(0) - \alpha > 0$. Therefore, Olech theorem proves that (Y^*, Z_p^*) is globally asymptotically stable. ■

Proof of Lemma 11: We arbitrarily choose

$$(\tilde{\theta}, \tilde{\xi}) \in]0, \mu_2[\times]\mu_1, 1 - \alpha[$$

and define the following closed set.

$$\Omega_\varepsilon(\tilde{\theta}, \tilde{\xi}) \equiv [Y(\tilde{\theta}), Y(\tilde{\xi})] \times [Y(\tilde{\theta}) - \varepsilon, Y(\tilde{\xi}) + \varepsilon].$$

Before proving Lemma 11, we prove the following four sublemmas.

Sublemma 1: For any $\varepsilon > 0$, $\Omega_\varepsilon(\tilde{\theta}, \tilde{\xi})$ is positively invariant. ■

Proof of Sublemma 1: First, we consider the direction of the vector field on $Y = Y(\tilde{\theta})$ ($< Y(\mu_2)$) and $Y = Y(\tilde{\xi})$ ($> Y(\mu_1)$). From the assumption of μ_2 and μ_1 , we see that for any $Z_p \in R^1$

$$\begin{aligned} \Theta(\beta(Y(\tilde{\theta}) - Z_p)) &\geq \inf\{\Theta(u) : u \in R^1\} = \mu_2 > \tilde{\theta}, \\ \Theta(\beta(Y(\tilde{\xi}) - Z_p)) &\leq \sup\{\Theta(u) : u \in R^1\} = \mu_1 < \tilde{\xi}. \end{aligned}$$

Therefore, from Lemma 5, we see that for any $Z_p \in R^1$,

(9.4.1) if $Y = Y(\tilde{\theta})$, then

$$\dot{Y} = \{\Theta(\beta(Y(\tilde{\theta}) - Z_p)) + \alpha - 1\}Y(\tilde{\theta}) + A > (\tilde{\theta} + \alpha - 1)Y(\tilde{\theta}) + A = 0, \text{ and}$$

(9.4.2) if $Y = Y(\tilde{\xi})$, then

$$\dot{Y} = \{\Theta(\beta(Y(\tilde{\xi}) - Z_p)) + \alpha - 1\}Y(\tilde{\xi}) + A < (\tilde{\xi} + \alpha - 1)Y(\tilde{\xi}) + A = 0.$$

Thus, we obtain

(9.5) if $(Y(0), Z_p(0)) \in [Y(\tilde{\theta}), Y(\tilde{\xi})] \times R^1$,

then $(Y(t), Z_p(t)) \in [Y(\tilde{\theta}), Y(\tilde{\xi})] \times R^1$ for any $t \geq 0$.

Next, choosing $\varepsilon > 0$ arbitrarily, we consider the direction of the vector field on $Z_p = Y(\tilde{\theta}) - \varepsilon$ or $Z_p = Y(\tilde{\xi}) + \varepsilon$. From the definition, for any $Y \in [Y(\tilde{\theta}), Y(\tilde{\xi})]$,

(9.6.1) if $Z_p = Y(\tilde{\theta}) - \varepsilon$, then $\dot{Z}_p = \beta\{Y - Y(\tilde{\theta}) + \varepsilon\} > 0$, and

(9.6.2) if $Z_p = Y(\tilde{\xi}) + \varepsilon$, then $\dot{Z}_p = \beta\{Y - Y(\tilde{\xi}) - \varepsilon\} < 0$.

Therefore, from (9.5) and (9.6), we see that

if $(Y(0), Z_p(0)) \in [Y(\tilde{\theta}), Y(\tilde{\xi})] \times [Y(\tilde{\theta}) - \varepsilon, Y(\tilde{\xi}) + \varepsilon]$,

then $(Y(t), Z_p(t)) \in [Y(\tilde{\theta}), Y(\tilde{\xi})] \times [Y(\tilde{\theta}) - \varepsilon, Y(\tilde{\xi}) + \varepsilon]$ for any $t \geq 0$.

This completes the proof of Sublemma 2. ■

Sublemma 2: $\bigcap_{\varepsilon>0} \Omega_\varepsilon(\tilde{\theta}, \tilde{\xi}) = \Omega_0(\tilde{\theta}, \tilde{\xi}) = \Omega(\tilde{\theta}, \tilde{\xi}).$ ■

Proof of Sublemma 2: From the definition, we have

$$\begin{aligned} \Delta &\equiv \bigcap_{\varepsilon>0} \Omega_\varepsilon(\tilde{\theta}, \tilde{\xi}) = \bigcap_{\varepsilon>0} [Y(\tilde{\theta}), Y(\tilde{\xi})] \times [Y(\tilde{\theta}) - \varepsilon, Y(\tilde{\xi}) + \varepsilon] \\ &= [Y(\tilde{\theta}), Y(\tilde{\xi})] \times [Y(\tilde{\theta}), Y(\tilde{\xi})] = \Omega_0(\tilde{\theta}, \tilde{\xi}) = \Omega(\tilde{\theta}, \tilde{\xi}). \end{aligned}$$

This completes the proof. ■

Sublemma 3: $\Omega(\tilde{\theta}, \tilde{\xi})$ is positively invariant. ■

Proof of Sublemma 3: We choose the solution $(Y(t), Z_p(t))$ starting from a point in $\Omega(\tilde{\theta}, \tilde{\xi})$ arbitrarily. We have $\Omega(\tilde{\theta}, \tilde{\xi}) \subseteq \Omega_\varepsilon(\tilde{\theta}, \tilde{\xi})$ for any $\varepsilon > 0$. From Sublemma 1, we have

$$(Y(t), Z_p(t)) \in \Omega_\varepsilon(\tilde{\theta}, \tilde{\xi}) \text{ for any } t \geq 0 \text{ and any } \varepsilon > 0.$$

Therefore, we find that for any $t \geq 0$,

$$(9.7) \quad (Y(t), Z_p(t)) \in \bigcap_{\varepsilon>0} \Omega_\varepsilon(\tilde{\theta}, \tilde{\xi}).$$

Thus, from (9.7) and Sublemma 2, for any $t \geq 0$ we have $(Y(t), Z_p(t)) \in \Omega(\tilde{\theta}, \tilde{\xi})$. This completes the proof of Sublemma 3. ■

Sublemma 4: $\Omega(\mu_2, \mu_1)$ is positively invariant. ■

Proof of Sublemma 4: We assume that $\Omega(\mu_2, \mu_1)$ is not positively invariant, contrary to the sublemma. Then, there are a solution $(Y(t), Z_p(t))$ and a $T > 0$ such that

$$(Y(0), Z_p(0)) \in \Omega(\mu_2, \mu_1) \text{ and } (Y(T), Z_p(T)) \in \text{ext}\Omega(\mu_2, \mu_1).$$

Therefore, there are

$$(\theta_1, \xi_1) \in]0, \mu_2[\times]\mu_1, 1 - \alpha[\quad \text{and} \quad (\theta_2, \xi_2) \in]\theta_1, \mu_2[\times]\mu_1, \xi_1[$$

such that

$$(9.8.1) \quad (Y(T), Z_p(T)) \in \partial\Omega(\theta_1, \xi_1) \subseteq \text{ext}\Omega(\mu_2, \mu_1)$$

$$(9.8.2) \quad \Omega(\theta_2, \xi_2) \subseteq \text{int}\Omega(\theta_1, \xi_1).$$

From (9.8), we obtain

$$(9.9) \quad \partial\Omega(\theta_1, \xi_1) \subseteq \text{ext}\Omega(\theta_2, \xi_2).$$

From this, we have

$$(Y(0), Z_p(0)) \in \Omega(\mu_2, \mu_1) \subseteq \Omega(\theta_2, \xi_2).$$

Moreover, Sublemma 3 shows that $\Omega(\theta_2, \xi_2)$ is positively invariant. Therefore, we obtain

$$(9.10) \quad (Y(T), Z_p(T)) \in \Omega(\theta_2, \xi_2).$$

On the other hand, (9.8.1) and (9.9) show

$$(Y(T), Z_p(T)) \in \partial\Omega(\theta_1, \xi_1) \subseteq \text{ext}\Omega(\theta_2, \theta_2).$$

This contradicts (9.10). Thus, we complete the proof of Sublemma 4. ■

We now start to prove Lemma 11. Let

$$(9.11) \quad (Y(0), Z_p(0)) \in \text{ext}\Omega(\mu_2, \mu_1).$$

Then, there is a

$$(\tilde{\theta}, \tilde{\xi}) \in]0, \mu_2[\times]\mu_1, 1 - \alpha[\quad \text{such that} \quad (Y(0), Z_p(0)) \in \Omega(\tilde{\theta}, \tilde{\xi}).$$

Therefore, from Sublemma 3, we see that the set $P \equiv \{(Y(t), Z_p(t)) : t \geq 0\}$ is bounded. Then, L_ω is a non-empty, bounded, and connected set¹¹. Let us prove the following.

$$(9.12) \quad L_\omega \cap \partial\Omega(\mu_2, \mu_1) \neq \phi.$$

Conversely, if $L_\omega \cap \partial\Omega(\mu_2, \mu_1) = \phi$, then (9.10) yield $L_\omega \subseteq \text{ext}\Omega(\mu_2, \mu_1)$. Since $(Y^*, Z_p^*) \in \text{int}\Omega(\mu_2, \mu_1)$, L_ω does not contain the equilibrium point. Therefore, from the Poincaré-Bendixson theorem, L_ω is a periodic path. On the other hand, (9.12) shows that there exists $(\theta_1, \xi_1) \in]0, \mu_2[\times]\mu_1, 1 - \alpha[$ such that

$$(9.13) \quad L_\omega \cap \partial\Omega(\theta_1, \xi_1) \neq \phi.$$

Moreover, (9.4) shows that L_ω enters $\text{int}\Omega(\theta_1, \xi_1)$. Then, there is a $(\theta_2, \xi_2) \in]\theta_1, \mu_2[\times]\mu_1, \xi_1[$ such that

$$(9.14) \quad \Omega(\theta_2, \xi_2) \subseteq \text{int}\Omega(\theta_1, \xi_1) \quad \text{and} \quad L_\omega \cap \Omega(\theta_2, \xi_2) \neq \phi.$$

Since according to Sublemma 3, $\Omega(\theta_2, \xi_2)$ is positively invariant and L_ω is a periodic path, from (9.14) it directly follows that $L_\omega \subseteq \Omega(\theta_2, \xi_2)$. Therefore, from (9.14), we obtain

$$\phi = L_\omega \cap \text{ext}\Omega(\theta_2, \xi_2) \supseteq L_\omega \cap \partial\Omega(\theta_1, \xi_1).$$

This contradicts (9.13). Thus, we prove (9.12). Sublemma 4 shows that $\Omega(\mu_2, \mu_1)$ is positively invariant. Therefore, (9.12) yields

$$L_\omega \subseteq \Omega(\mu_2, \mu_1).$$

This completes the proof of Lemma 11. ■

Proof of Theorem 1: From (9.3) and Assumptions 7 and 8, we obtain

¹¹ For this point, see Wiggins (1990, Section 1.1)

$$(9.15.1) \quad \text{tr}J(Y^*, Z_p^*) = \frac{A\Theta'(0)}{1-\alpha-\Theta(0)} + \Theta(0) + \alpha - 2 > 0,$$

$$(9.15.2) \quad \det J(Y^*, Z_p^*) = -\left\{ \frac{A\Theta'(0)}{1-\alpha-\Theta(0)} + \Theta(0) + \alpha - 1 \right\} + \frac{A\Theta'(0)}{1-\alpha-\Theta(0)} \\ = -\{\Theta(0) + \alpha - 1\} > 0.$$

Thus, we obtain that the real parts of the eigenvalues of the Jacobian matrix (9.3) are positive. This completes the proof of Theorem 1. ■

Proof of Lemma 12: From a simple calculation, we obtain

$$\Theta(0) = a\text{Arctan}(c) + d \quad \text{and} \quad \Theta'(0) = ab/(c^2 + 1).$$

Therefore, from (9.15.1), we obtain

$$(9.16) \quad \text{tr}J(Y^*, Z_p^*) = \frac{abA}{(c^2 + 1)(1 - \alpha - a\text{Arctan}(c) - d)} + a\text{Arctan}(c) + d + \alpha - 2 \\ = H(a, b, c, d, \alpha, A) - 2.$$

Thus, from (9.15.2) we obtain that the equilibrium point is completely unstable (resp. asymptotically stable) if and only if $\text{tr}J(Y^*, Z_p^*) > 0$ (resp. $\text{tr}J(Y^*, Z_p^*) < 0$). On the other hand, $\text{tr}J(Y^*, Z_p^*) > 0$ (resp. $\text{tr}J(Y^*, Z_p^*) < 0$) if and only if

$$H(a, b, c, d, \alpha, A) > 2 \quad (\text{resp. } H(a, b, c, d, \alpha, A) < 2).$$

We see from (9.15.1) that $\text{tr}J(Y^*, Z_p^*) > 0$ is equivalent to Assumption 9. Thus, we complete the proof. ■

Proof of Lemma 13: We arbitrarily choose $c \in [c_1, c_2] = [-3.0054, -2.992]$. A simple calculation yields

$$(9.17) \quad H(0.03/\pi, 1/100, c, 0.1, 0.8, 9900) \\ = \frac{0.03 \cdot 99/\pi}{(c^2 + 1)\{0.08 - (0.03/\pi)\text{ArcTan}(c)\}} + (0.03/\pi)\text{ArcTan}(c) + 0.92.$$

We see that

- (9.18.1) $(0.03/\pi)\text{ArcTan}(c) < 0.009\text{ArcTan}(-2.992) < 0$,
(9.18.2) $0.08 - (0.03/\pi)\text{ArcTan}(c) > 0.08 - 0.009\text{ArcTan}(-2.992) > 0$,
(9.18.3) $-1.25 < \text{ArcTan}(-2.992) < -1.24$.

Therefore, (9.17) and (9.18) yield

$$\begin{aligned}
& H(0.03/\pi, 1/100, c, 0.1, 0.82, 9900) \\
& < \frac{2.97/\pi}{(3.0053^2 + 1)\{0.08 - 0.01\text{ArcTan}(-2.992)\}} + 0.009\text{ArcTan}(-2.992) + 0.92 \\
& < \frac{0.9454}{10\{0.08 - 0.009\text{ArcTan}(-2.992)\}} + 0.009\text{ArcTan}(-2.992) + 0.92 \\
& < \frac{0.9454}{10\{0.08 + 0.009 \bullet 1.25\}} - 0.009 \bullet 1.24 + 0.92 < 1.95 < 2.
\end{aligned}$$

Thus, Lemma 12 proves that the equilibrium point is asymptotically stable. ■

Acknowledgment

This paper is dedicated to the late Tatsuji Owase. His remarkable book that stresses the importance of nonlinear science led us into the profound forest of nonlinear economic dynamics.

References

- Asada, T., 1989. Government finance and wealth effect in a Kaldorian cycle model. *Journal of Economics* 47, 143-166.
- Benhabib, J., Miyao, T., 1981. Some New Results on the Dynamics of the Generalized Tobin Model. *International Economic Review* 22, 589-596.
- Chang, W.W., Smyth, D.J., 1971. The existence and persistence of cycles in a non-linear model: Kaldor's 1940 model re-examined. *Review of Economic Studies* 38, 37-44.
- Gabisch, G., Lorenz, H.-W., 1989. *Business Cycle Theory-A Survey of Methods and Concepts*. Second ed. Berlin: Springer-Verlag.

- Gandolfo, G., 1996. *Economic Dynamics*. Third, Completely Revised and Enlarged Edition.
- Glendinning, P., 1994. *Stability, Instability and Chaos: An Introduction to the Theory of Nonlinear Differential Equations*. Cambridge: Cambridge University Press.
- Goodwin, R.M., 1951. The Nonlinear Accelerator and the Persistence of Business Cycles. *Econometrica* 19, 1-17.
- Guckenheimer, J., Holmes, P., 1983. *Nonlinear Oscillations, Dynamical Systems, and Bifurcations of Vector Fields*. New York: Springer-Verlag.
- Kaldor, N., 1940. A Model of the Trade Cycle. *Economic Journal* 50, 78-92 (reprinted in *Essays on Economic Stability and Growth*, 1964. Duckworth, London, pp. 177-192).
- Kalecki, M., 1945., On the Gibrat distribution. *Econometrica* 13, 161-170.
- Keynes, J.M., 1936. *The General Theory of Employment, Interest and Money*. London: Macmillan.
- Kuznetsov, Y.A., 1995. *Elements of Applied Bifurcation Theory*. New York-Berlin-Heidelberg: Springer-Verlag.
- Leijonhufvud, A., 1973. Effective Demand Failure. *Swedish Journal of Economics* 75, 27-48.
- Lorenz, H.-W., 1993. *Nonlinear Dynamical Economics and Chaotic Motion*. Berlin-Heidelberg-New York: Springer-Verlag.
- Mandelbrot, B., 1960, The Pareto-Levy law and the distribution of income. *International Economic Review* 1, 79-106.
- Medio, A., Lines, M., 2001. *Nonlinear Dynamics*. Cambridge: Cambridge University Press.
- Olech, C., 1963. On the global stability of an autonomous system on the plane. In: Lasalle, P., Diaz P. (Eds), *Contributions to Differential Equations* 1, John Wiley & Sons, New York, 389–400.
- Owase, T., 1991. Nonlinear Dynamical Systems and Economic Fluctuations: A Brief Historical Survey. *IEICE Transactions* 74, 1393-1400.
- Perko, L., 1996. *Differential Equations and Dynamical Systems*, Second Edition. New York: Springer-Verlag.
- Pontryagin, L.S., 1962. *Ordinary Differential Equations*. London: Addison-Wesley.
- Simon H. A., 1955. On a class of skew distribution functions. *Biometrika* 42, 425-440.
- Wiggins, S., 1990. *Introduction to Applied Nonlinear Dynamical Systems and Chaos*. New York: Springer-Verlag.

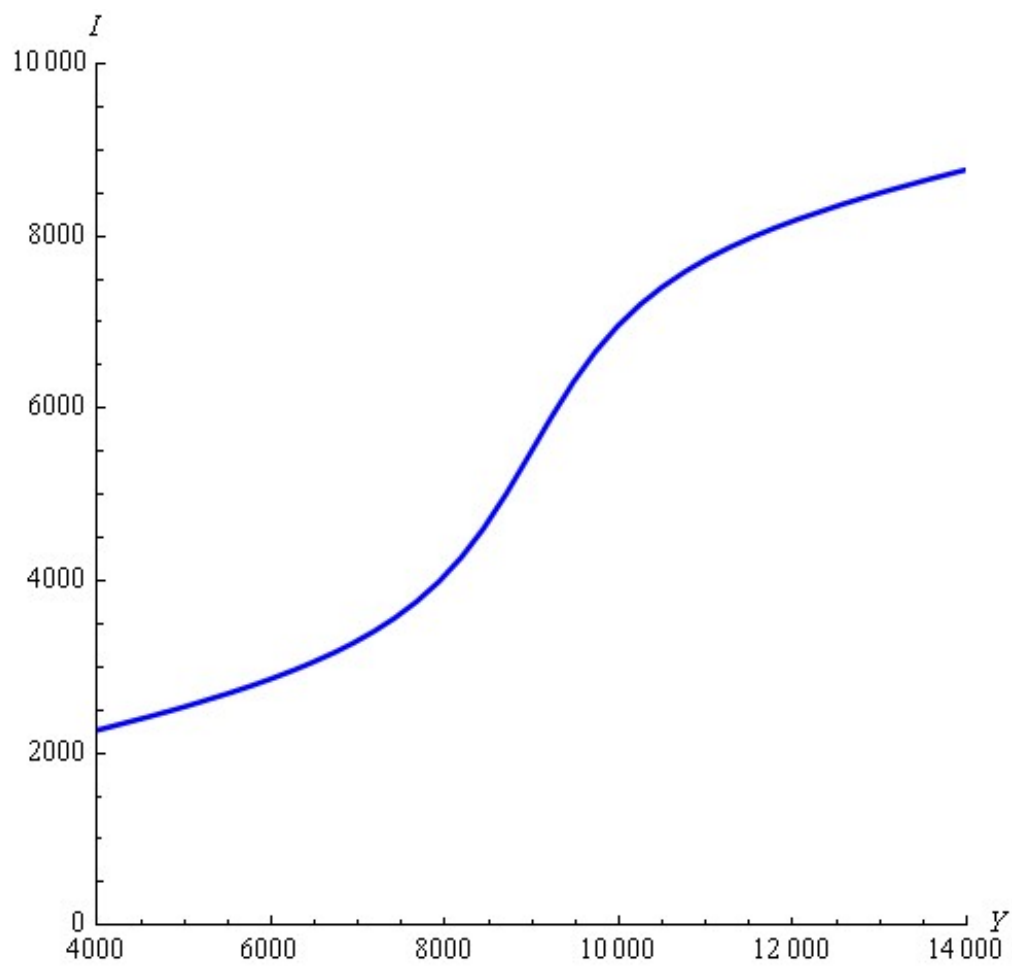


Figure 1

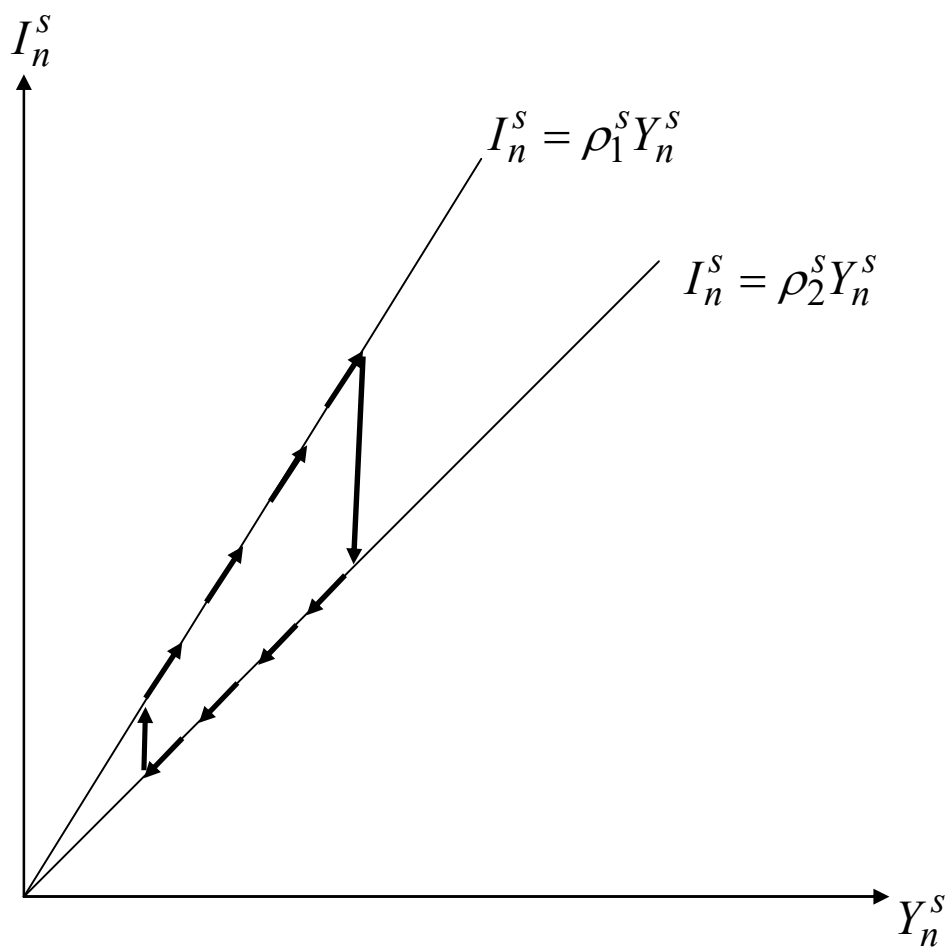
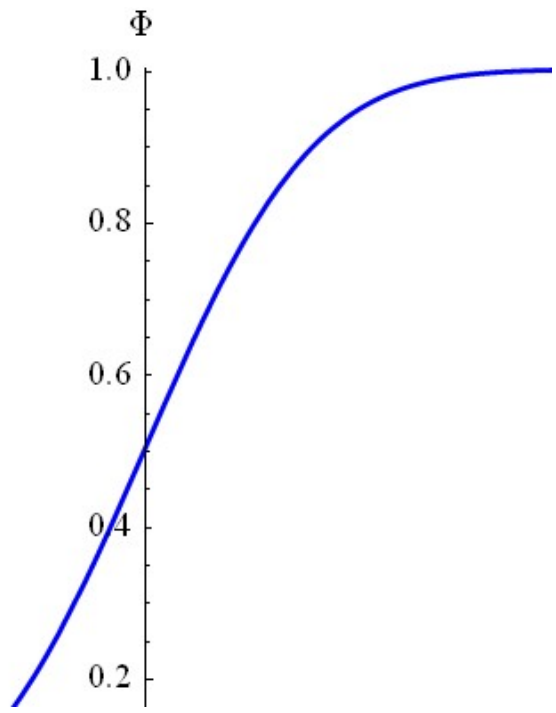
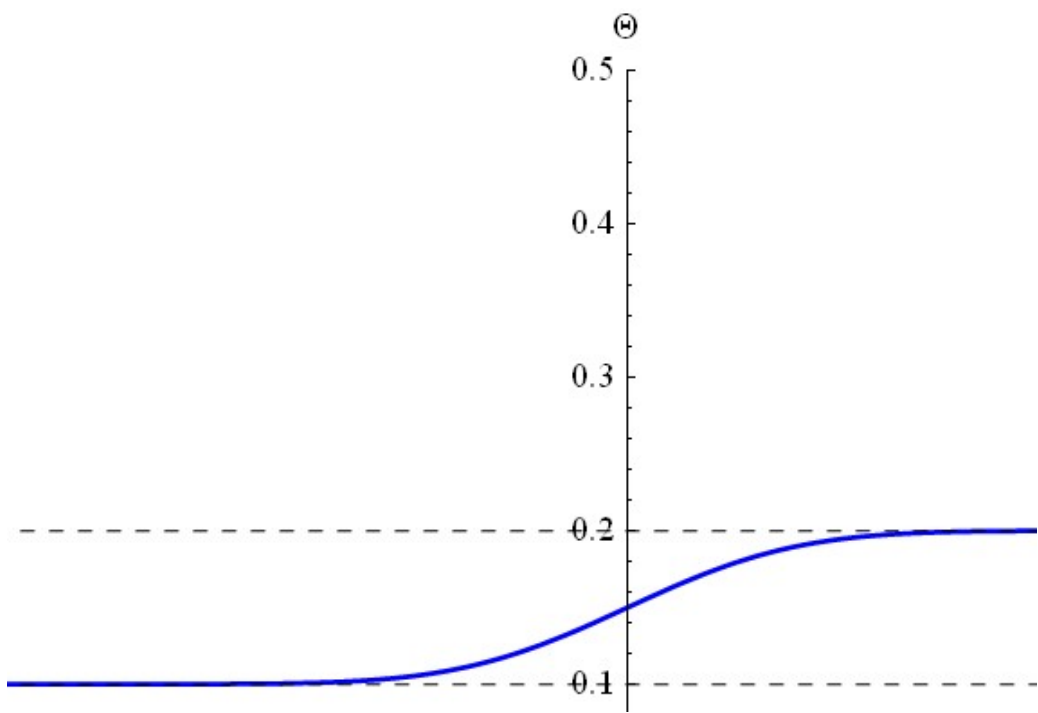


Figure 2



(1)



(2)

Figure 3

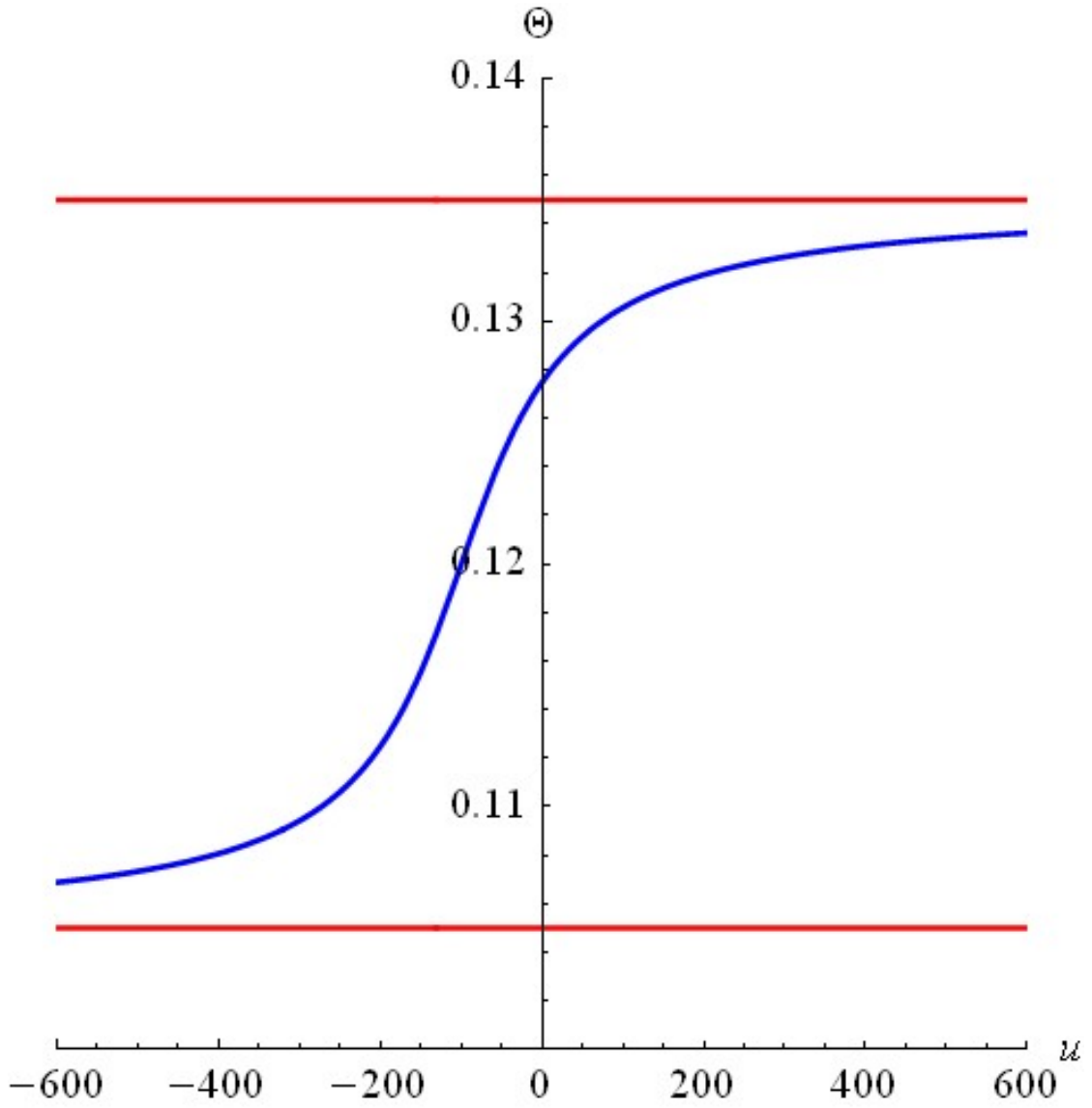


Figure 4

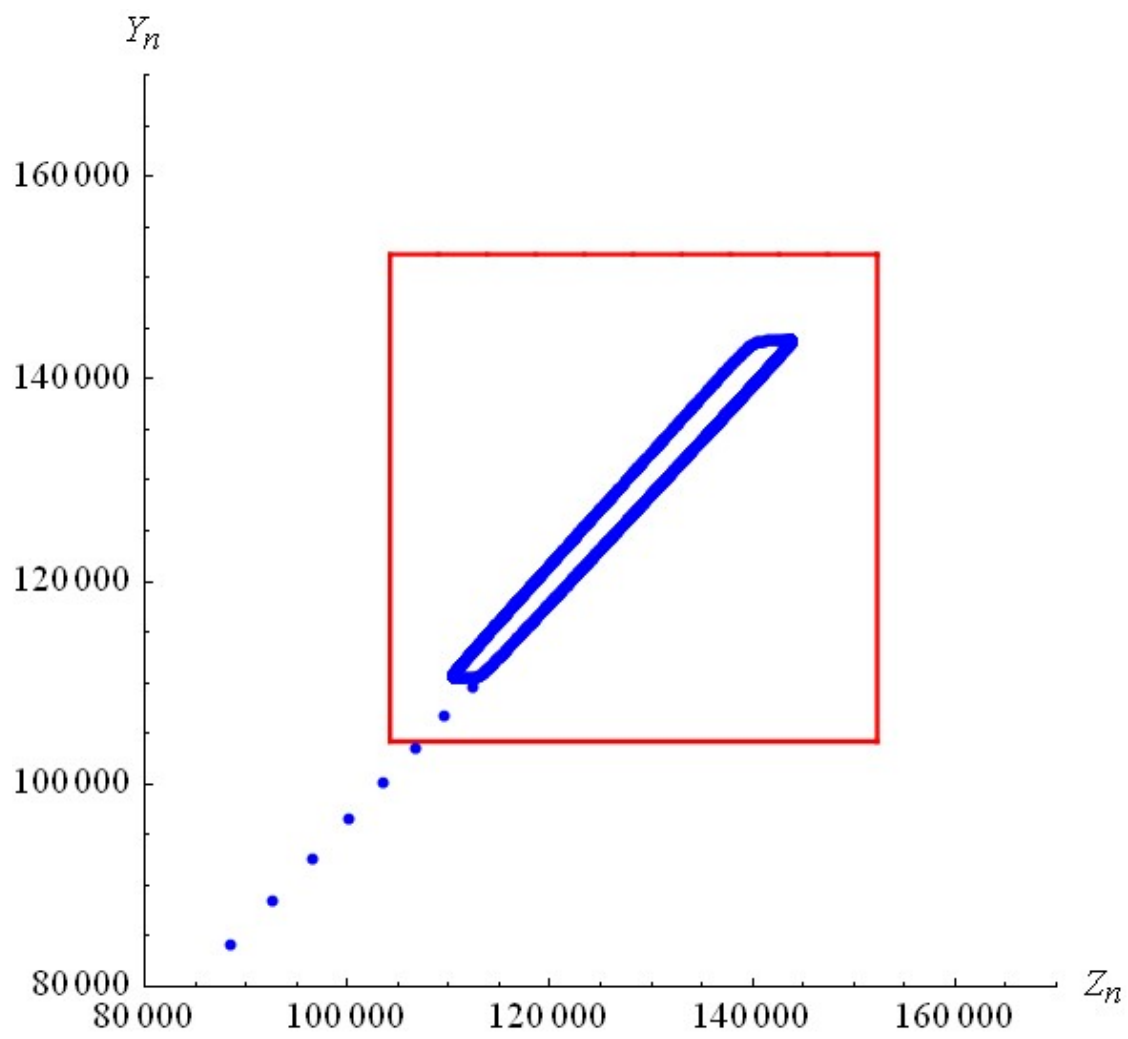


Figure 5

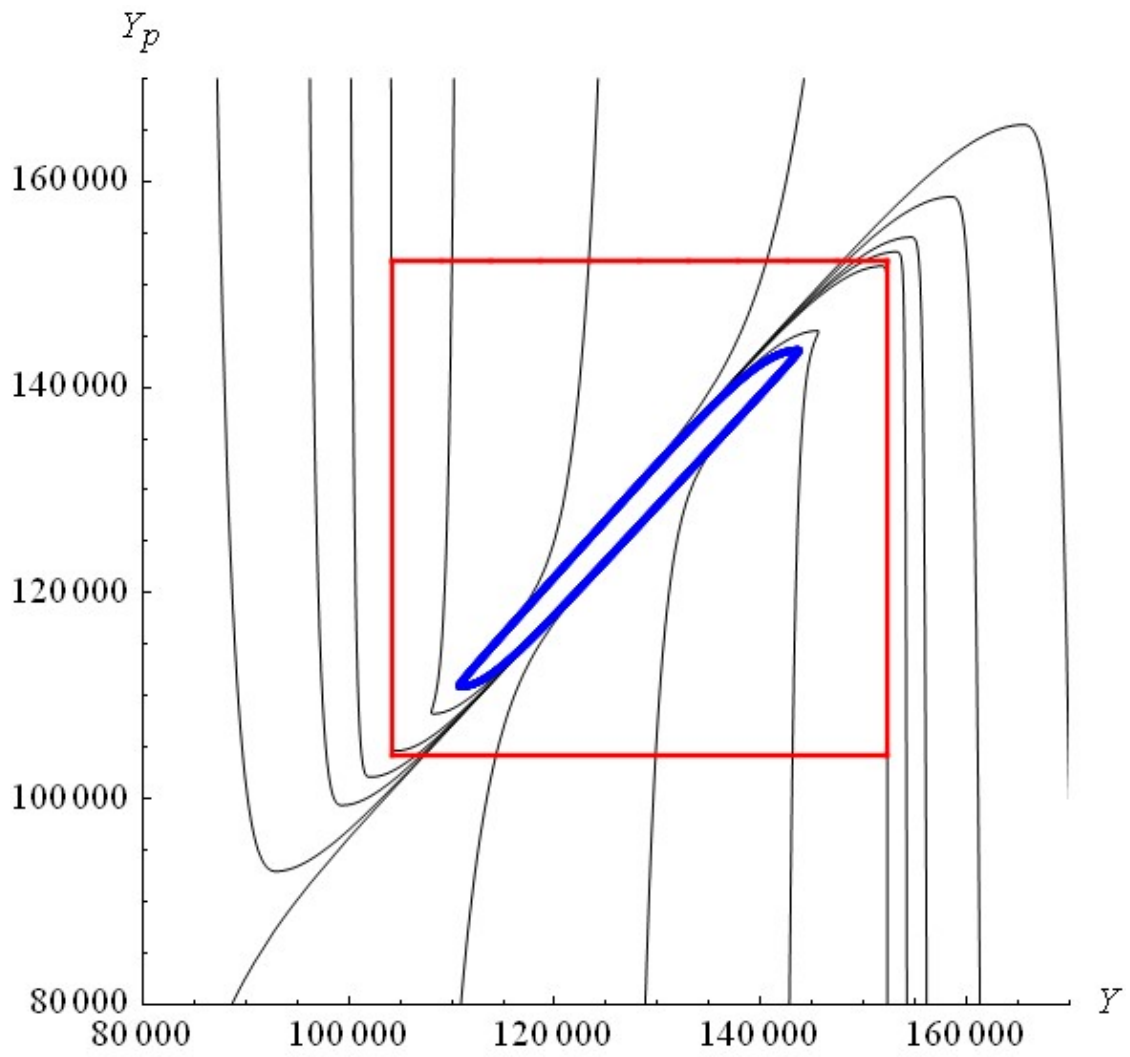
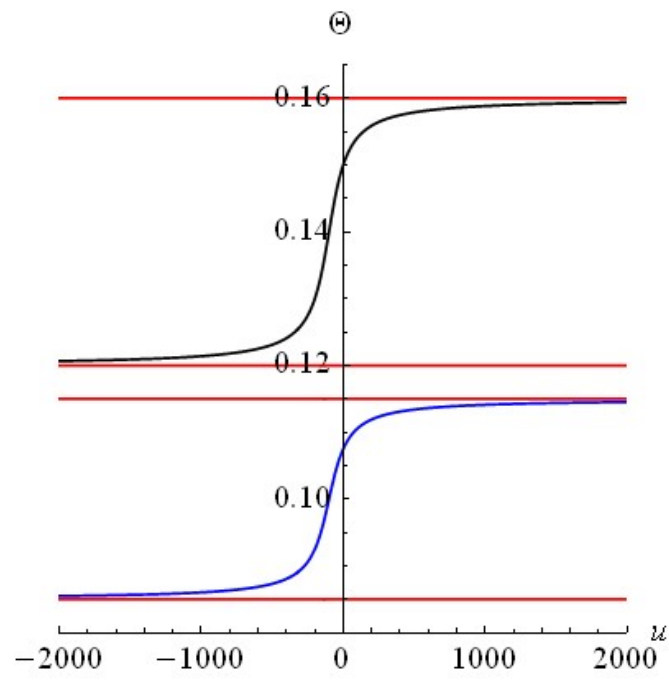
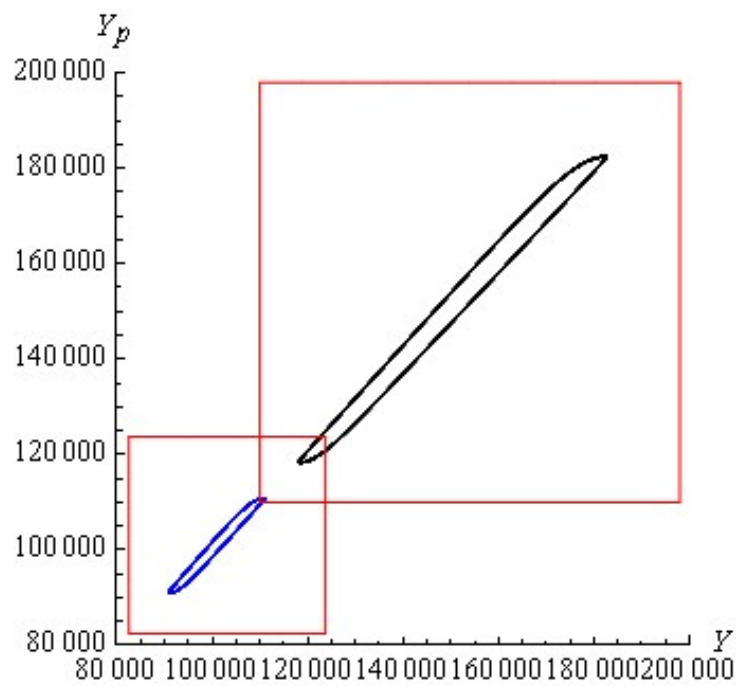


Figure 6



(1)



(2)

Figure 7

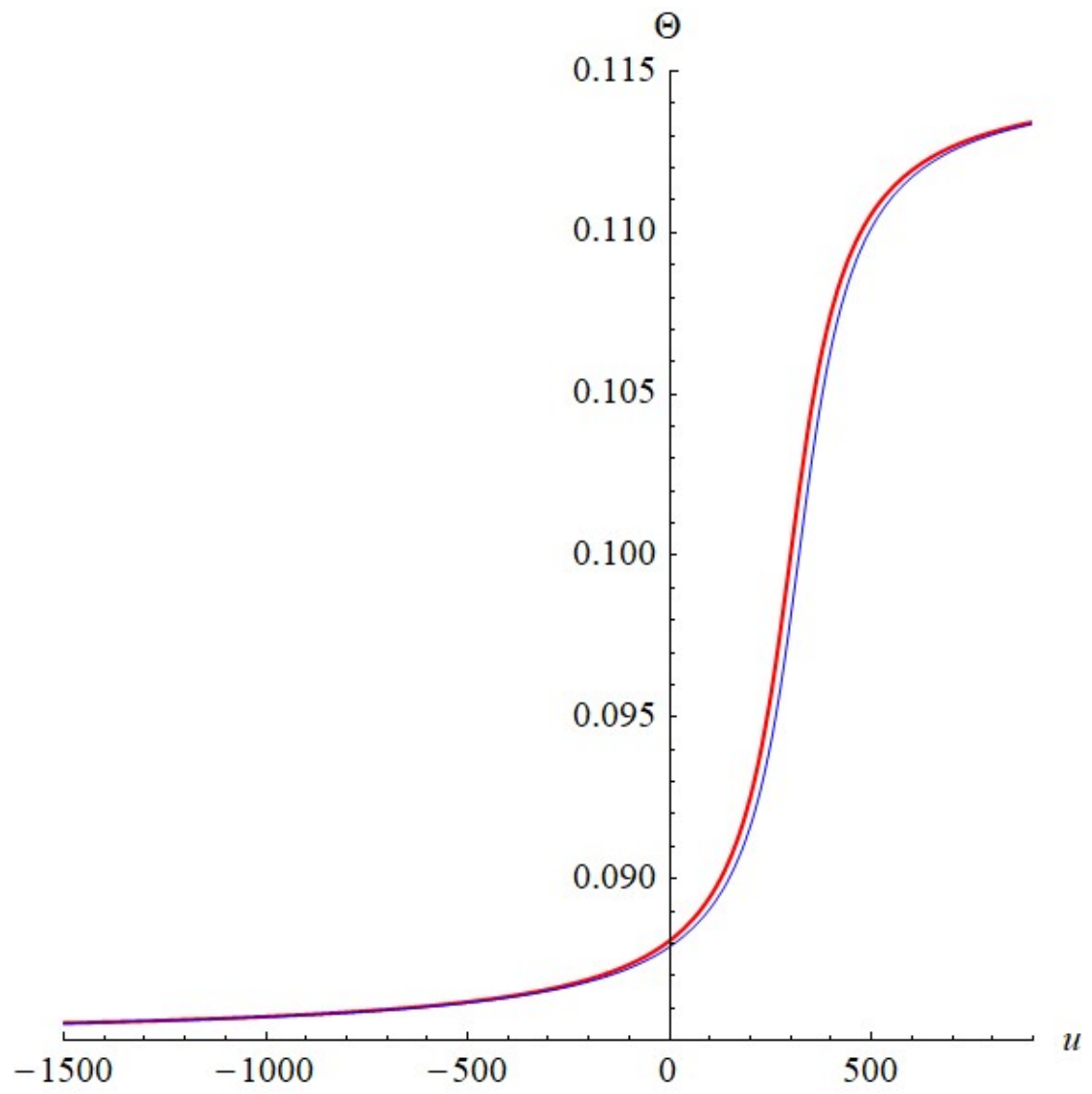
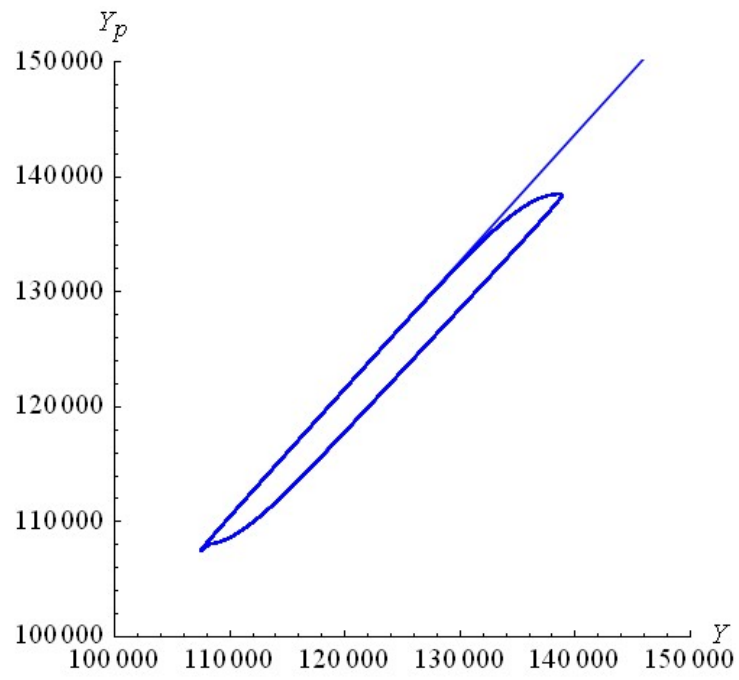
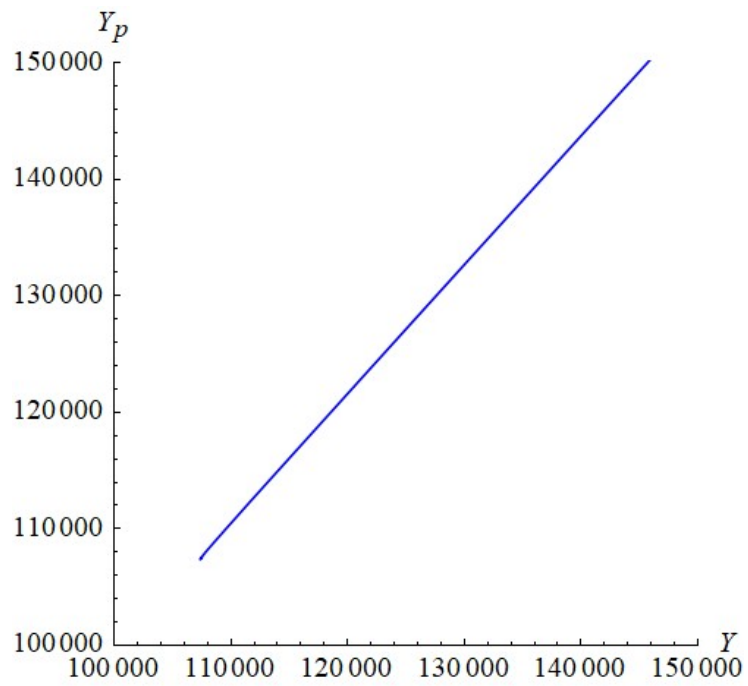


Figure 8



(1)



(2)

Figure 9

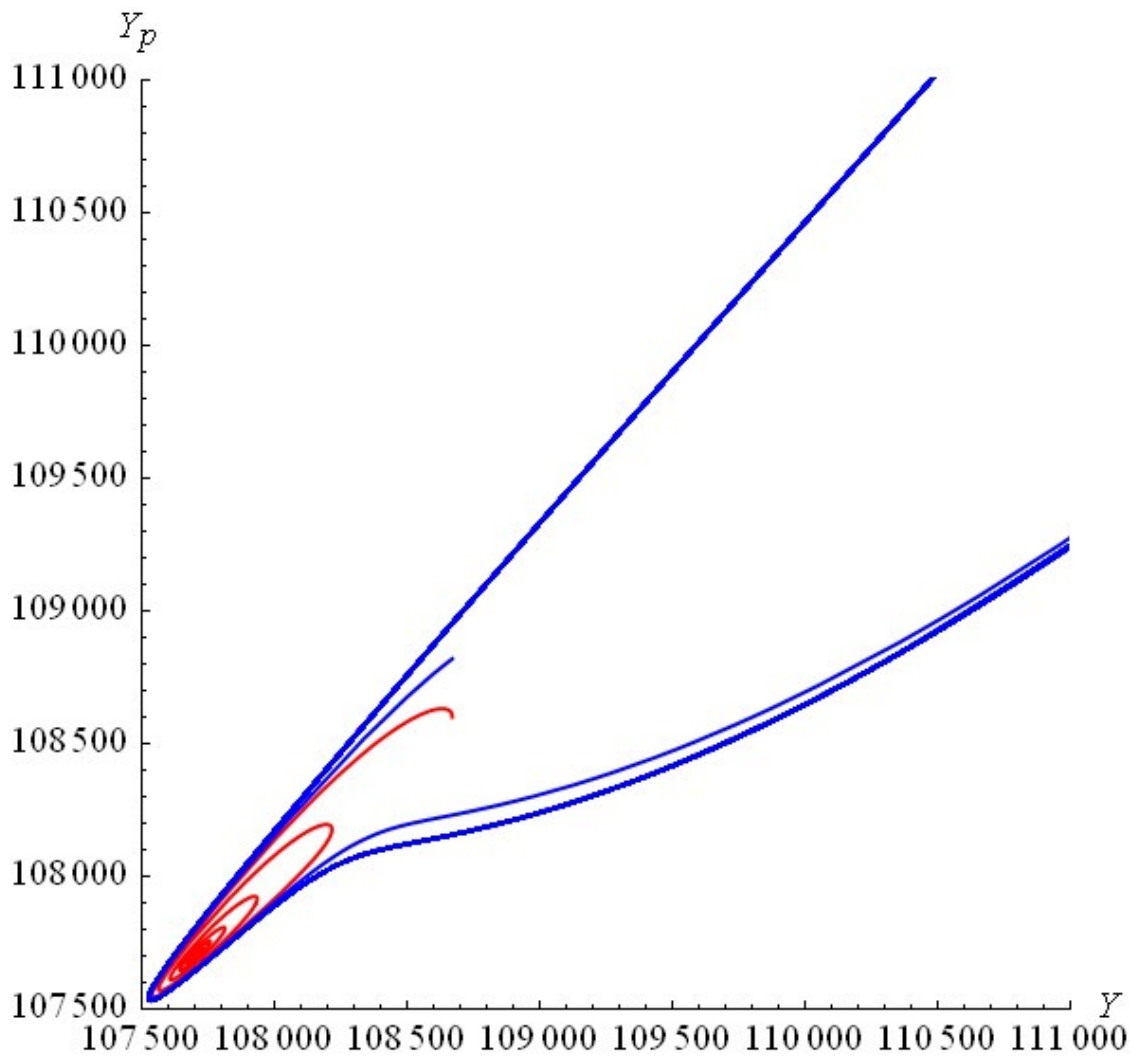


Figure 10

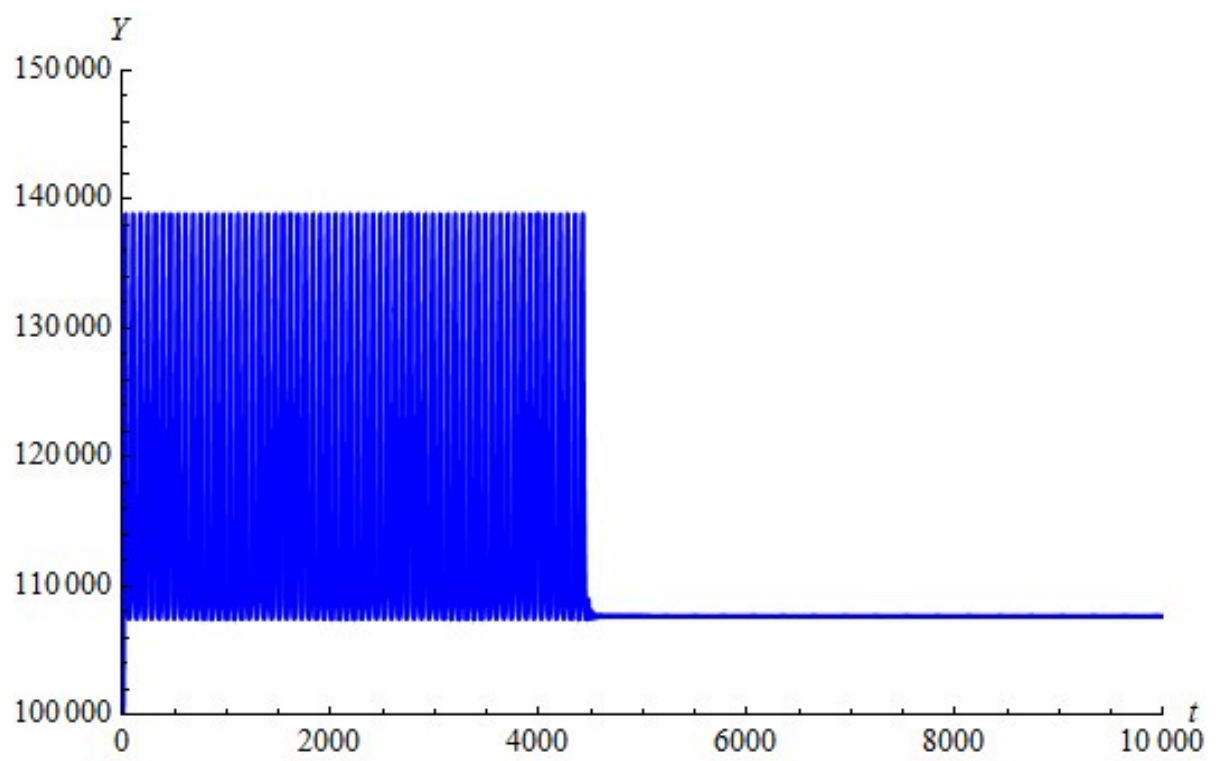
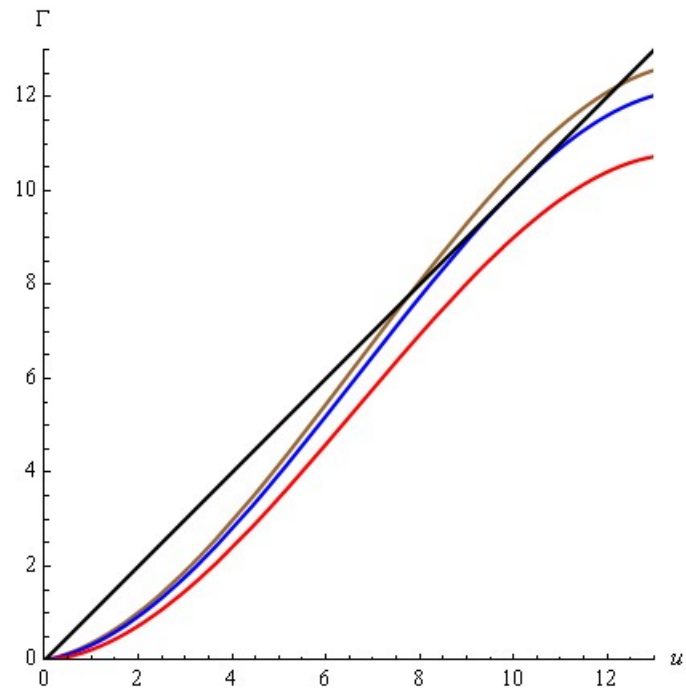
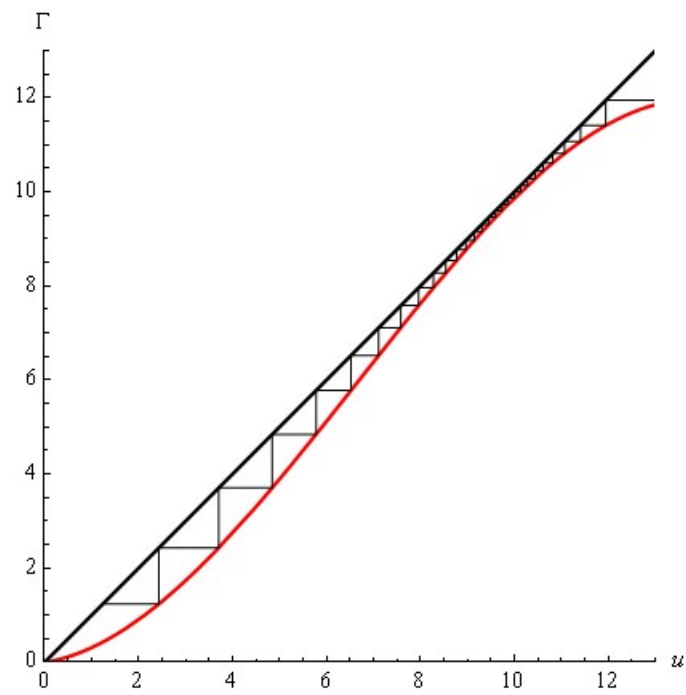


Figure 11

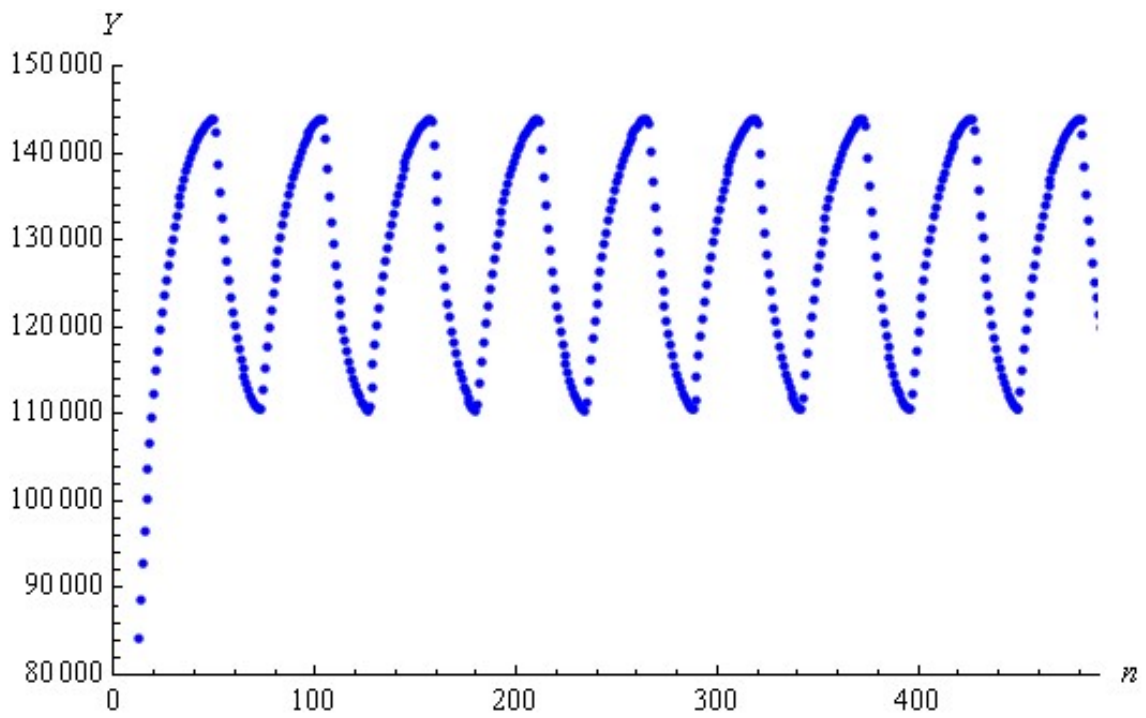


(1)

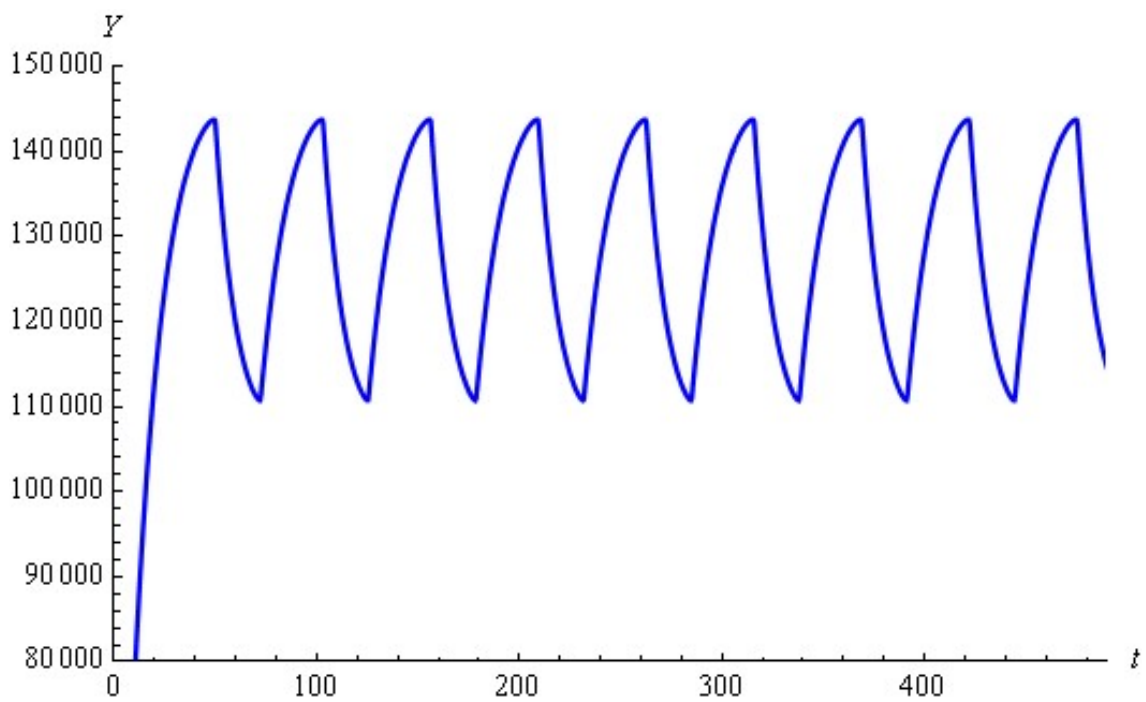


(2)

Figure 12

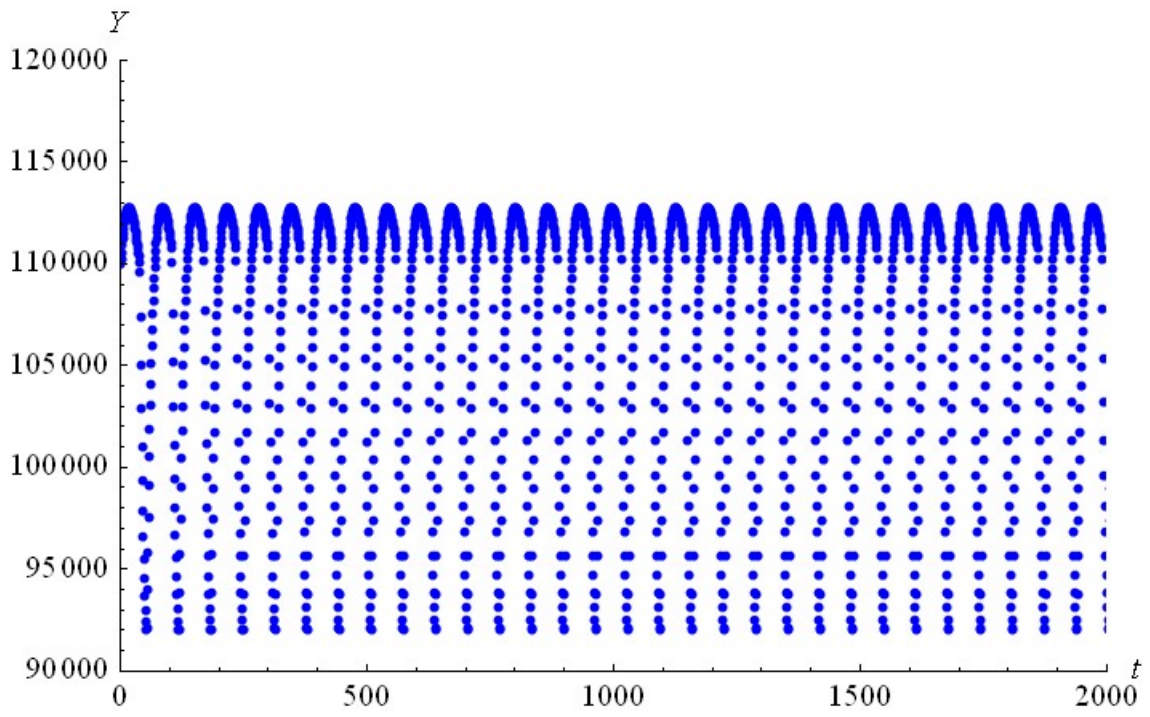


(1)

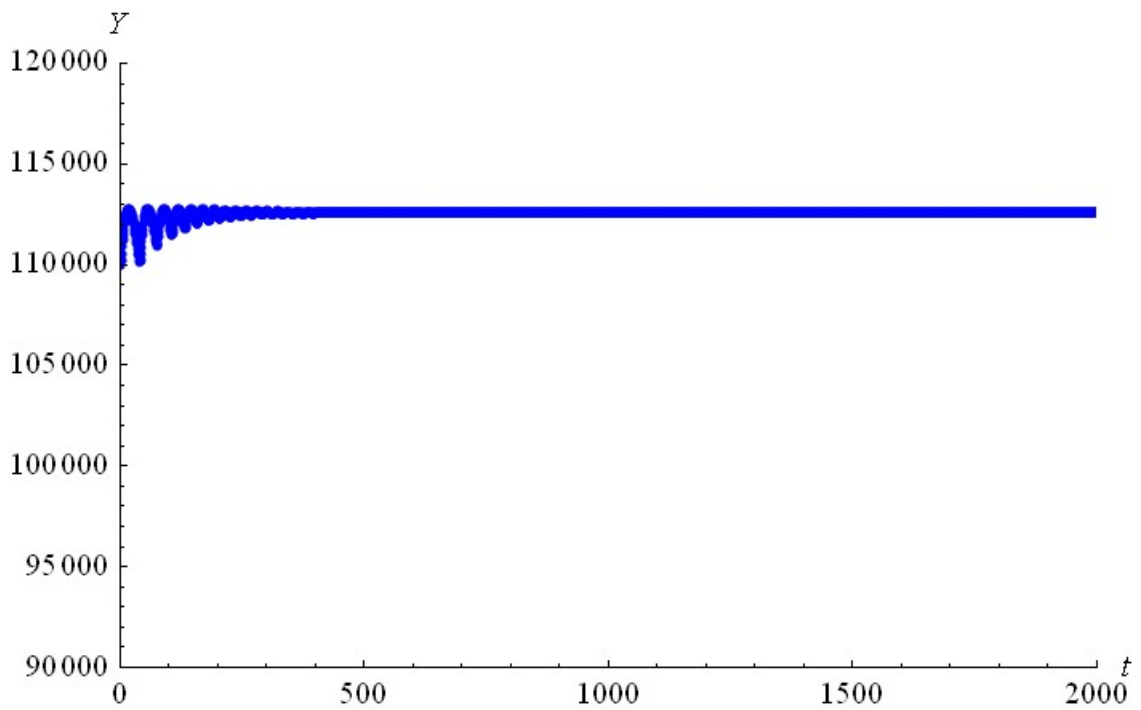


(2)

Figure 13



(1)



(2)

Figure 14